Algorithms for Stackelberg Security Games

Renaud Chicoisne, Fernando Ordóñez

Mathematical Programming, Series B manuscript No.
(will be inserted by the editor)

Algorithms for Stackelberg Security Games

Renaud Chicoisne · Fernando Ordóñez

Received: date / Accepted: date

Abstract In a basic Stackelberg security game (SSG), a defender can simultaneously protect m out of n targets with $n > m$ from an adversary that observes the defense strategy and attacks where most convenient for him. We consider a more realistic model where 1) The defender faces several different opponents, 2) The adversaries are not completely rational and follow a quantal response (QR) to decide which target to attack, and 3) We introduce risk aversion in the defender's behavior by minimizing an entropic risk measure instead of an expected loss.

Our contribution is as follows: 1) We show that we can find the risk-minimizing defense policy by solving a nonconvex nonlinear optimization problem, 2) We present an approximated problem (MINR) tailored for SSG that is a convex mixed Integer nonlinear program, 3) We propose a general purpose methodology (CELL) to optimize nonconvex and nonseparable fractional programming problems via Mixed Integer linear Programming (MIP) approximations, 4) We show that both problems provide lower bounds for SSG as well as arbitrarily good incumbents, and 5) We present cutting plane methods to solve them to optimality with an off the shelf MIP solver.

We test both algorithms on a large bedset of mid-sized instances and show that MINR clearly dominates CELL and is able to produce - on average - solutions that are within 2% of optimality in 2 hours. We finish by showing the empirical qualitative advantages of introducing risk aversion into the defender's behavior.

Keywords Stackelberg Security Games, Risk Averse Optimization, Entropic Risk Measure, Quantal Response, Piecewise Linear Approximation, Decomposition

R. Chicoisne
Université Libre de Bruxelles
Boulevard du Triomphe
Brussels, Belgium
E-mail: renaud.chicoisne@gmail.com

F. Ordóñez
Universidad de Chile
Beauchef 850
Santiago, Chile
E-mail: fordon@dii.uchile.cl

1 Introduction

In this work we develop efficient solution methods for a fractional nonconvex optimization problem motivated from a Stackelberg game model in security applications. A Stackelberg game is defined as a game where the leader decides a mixed strategy to maximize its utility, taking into account that the follower will observe this strategy and in turn decide the action to maximize its utility [25]. In particular, Stackelberg game models have been used to represent the interaction between defenders (that act as the leader) and attackers (corresponding to followers) in diverse security settings [3,4,12]. For example, when defenders must patrol a subset of targets and each adversary - knowing the patrolling strategy - selects the target to attack [16,13]. Examples of such Stackelberg security games have been successfully deployed in real-world security applications to help plan the patrols conducted by the Los Angeles International Airport Police on LAX [16], the US Federal Air Marshal Service on transatlantic flights [23], the LA Sheriff department on Los Angeles' subway system [11], and the US Coast Guard on ports and waterways in Boston and New York City [20].

The Stackelberg security game model we investigate, which appears in [27,6], makes two additional considerations: 1) it assumes adversaries use a logit discrete choice model to select their action, and 2) the leader includes risk considerations on its objective function, optimizing an entropic risk measure objective.

Stackelberg games typically assume a perfectly rational attacker that maximizes its utility knowing the defense strategy [16,13], or that can deviate slightly from the optimal attack [17]. Nevertheless, humans sometimes make decisions that are different from the policy that optimizes a given reward function [5]. Consequently, assuming a highly intelligent adversary can lead to weak defense strategies, that fail to take advantage of our knowledge about the attacker. The Quantal Response (QR) Equilibrium model presented in [15] assumes that human adversaries do not behave rationally, sometimes selecting actions that do not maximize their utility. In this model, followers use a logit discrete choice model to decide between n possible actions, where action i (that gives a payoff U_i) is selected with probability:

$$\mathbb{P}(\text{selecting action } i) = \frac{1}{\sum_{j=1}^{n} e^{\lambda U_j}} e^{\lambda U_i} \ ,$$

where the parameter λ represents a *degree of rationality*, with perfect rationality ($\lambda \to \infty$) or indifference ($\lambda = 0$) as special cases. This QR model has been shown in diverse settings (including security applications) to more closely model human behavior [9,21,26,27].

In a security domain, the consequences of catastrophic unlikely events could far outweigh that of more common occurrences. However, planning for the worst case can dedicate resources for scenarios that rarely occur, while planning for the expected outcome could divert key resources from the catastrophic events. Different risk measures have been used to balance likely outcomes with rare but catastrophic ones in decision models. In this work, we use an Entropic risk measure [18] that amplifies the importance of outcomes that exceed a given threshold. The entropic risk measure of parameter $\alpha > 0$ of a random variable Y is defined by $\alpha \ln \mathbb{E}\left[e^{\frac{Y}{\alpha}}\right]$. While all outcomes are weighted, scenarios with a payoff larger than α contribute more to this measure. Therefore, the parameter α corresponds to

a payoff value of risky outcomes and must be chosen carefully to tune the risk aversion level of the decision maker. Consider now the following example that shows the effect of using the expected value objective (of optimal solution x^*) or the entropic measure objective (of optimal solution $\tilde{x}$) on a small example where there are two targets, a single patrol, and a single attacker with rationality factor $\lambda = 0.25$. The payoffs of this game (were the defender is the row player and the attacker is the column player) are given in Table 1a.

	attack 1	attack 2
patrol 1	3, -1	-3, 1
patrol 2	-1, 3	1, -3

(a) Payoffs matrix. Each cell gives defender utility, attacker utility.

	$\mathbb{E}$	$\mathbb{V}$	w.c. $\mathbb{P}$
x^*	0.245	4.980	0.192
$\tilde{x}$	0.233	4.546	0.159
Diff.	-4.9%	-8.7%	-16.9%

(b) Comparing x^*, $\tilde{x}$ on expected value, variance and worst case probability.

Table 1: Two targets, one defender resource example

Both the expected utility objective problem and the entropic risk measure problem for this example can be expressed as a single variable non-linear problem that can be solved numerically (presented in Section 2), giving the results summarized in Table 1b. The solution that optimizes the entropic risk measure, $\tilde{x}$, has a smaller variance and a smaller probability of the worst case scenario than the solution that optimizes the expected value, x^*. Using an Entropic risk measure gives a solution that reduces the possible bad outcomes, thus reducing the variance that the solution observes at the expense of a worse expected value.

Stackelberg security game models with a quantal response adversary were introduced in [28] for the case of a single adversary, leading to problems with the following structure:

$$\begin{aligned} \min_{x} \ & \frac{1}{\sum_{i=1}^{n} \beta_i e^{-\gamma_i x_i}} \sum_{i=1}^{n} \beta_i e^{-\gamma_i x_i} \left(a_i - b_i x_i\right) \\ \text{s.t.} \ & Hx \leq h \ . \end{aligned}$$

That work used a binary search procedure on the fractional objective to provide an approximate solution by solving a polynomial number of optimization problems. Furthermore they showed that if the defender strategy only has resource constraints, a non-linear transformation makes these optimizations problems convex. In the case of additional constraints, a piecewise linear approximation turns these optimization problems into mixed linear optimization problems. This line of work is extended in [6] by considering the use of an entropic risk measure for the single follower case. The authors show that the problem maintains the above structure and extend the convex reformulation to the case where the defender strategy has linear constraints with a positive coefficient matrix.

To the best of our knowledge there is no prior work on Stackelberg security games with quantal response for multiple followers. Given that multiple adversaries in Stackelberg games are modeled using a Bayesian model [10], considering multiple adversaries is equivalent to considering uncertainty in the payoff functions. This

makes the multiple follower problem a stochastic version of the single follower problem introduced in [28,6]. In this work we develop efficient solution methods for the stochastic Stackelberg game with quantal response followers, which considers algorithms for problems with the following form:

$$\begin{aligned} \min \sum_{l=1}^{p} \pi^l \frac{1}{\sum_{i=1}^{n} \beta_i^l e^{-\gamma_i^l x_i}} \sum_{i=1}^{n} \beta_i^l e^{-\gamma_i^l x_i} \left(a_i^l - b_i^l x_i\right) \\ \text{s.t. } Hx \leq h \ , \end{aligned} \tag{1}$$

with non-negative coefficients β_i^l, γ_i^l, a_i^l, and b_i^l.

In this work we propose two different solution strategies to approximately solve the stochastic problem above in the case of general polyhedral constraints. The first recasts the problem as a nonconvex nonlinear optimization problem that we can approximate via piecewise linear approximations. The second uses a generic methodology to approximate multidimensional nonlinear functions via spatial discretization. Both solution strategies require efficiently solving the mixed integer linear optimization problems that arise. We structure the rest of the paper as follows: in the next section we introduce the problem formulation that will be considered in this paper. In Section 3 we present the solution methods that solve the Stackelberg security game with multiple quantal response followers and show that both can provide arbitrarily good defense strategies. In Section 4 we present repair heuristics for both models and strategies to select the discretization points in order to speed up the solution methods and strenghten the relaxation bounds. We show experimental results in Section 5 on mid-sized artificial instances and compare the performance of our algorithms and the quality of the solution they provide. We present our conclusions in Section 6.

2 Notation and problem formulation

The Stackelberg security game we consider consists of a single leader (defender) that patrols n targets that could be attacked by one of p followers (attackers). The leader can patrol up to $m < n$ targets simultaneously and each follower selects one target to attack. The payoffs for the leader and the followers depend on whether the target attacked is patrolled or not. If follower $l \in \{1 \dots p\}$ attacks target $i \in \{1 \dots n\}$, then the payoffs received by attacker l are either a reward $R_i^l > 0$ if the target is not patrolled or a penalty $P_i^l < 0$ if the target is patrolled. Similarly, if attacker l attacks target i, we let the payoffs for the defender be a reward $\bar{R}_i^l > 0$ when the target is patrolled and a penalty $\bar{P}_i^l < 0$ if it is not patrolled.

The set of actions for the defender are the feasible subsets of targets $I \subseteq \{1, \dots, n\}$ that can be patrolled simultaneously ($|I| \leq m$). We denote by z the mixed strategy over this action space, so that z_I is the probability with which the defender patrols the set of targets I. Since the payoffs only depend on whether a target i is patrolled or not, we consider the frequency of protecting target i, given by $x_i = \sum_{i \in I} z_I$, the sum of probabilities of the defender strategies that patrol i. With the frequency of patrolling target i, $x_i \in [0, 1]$, we can express the expected utility of the defender and attacker l when target i is attacked by follower l as $\bar{U}_i^l(x_i) = x_i \bar{R}_i^l + (1 - x_i)\bar{P}_i^l$ and $U_i^l(x_i) = x_i P_i^l + (1 - x_i)R_i^l$, respectively.

Since follower $l \in \{1 \dots p\}$ selects targets according to a QR model with a rationality parameter $\lambda^l > 0$, we denote the probability of attacker l selecting target i by

$$y_i^l(x) = \frac{1}{\sum_{j=1}^{n} e^{\lambda^l U_j^l(x_j)}} e^{\lambda^l U_i^l(x_i)} = \frac{e^{\lambda^l (x_i P_i^l + (1-x_i) R_i^l)}}{\sum_{j=1}^{n} e^{\lambda^l (x_j P_j^l + (1-x_j) R_j^l)}} \ . \tag{2}$$

2.1 Expected utility defender problem

Similar to prior work on Stackelberg security games [13,28], we formulate the defender optimization problem in terms of this frequency variable, which by definition satisfies $x_i \in [0,1]$, and $\sum_{i=1}^{n} x_i \leq m$. We assume that the vector of frequency variables must satisfy a set of linear constraints $Hx \leq h$ that can represent additional constraints on feasible patrols (e.g. targets i and i' cannot (or must) be patrolled together). We denote $\mathcal{X} = \{x \ : \ Hx \leq h\}$ the feasible set of defender frequency variables. For an integer k, let $[k] := \{1, \dots, k\}$. Let π^l represent the probability of facing follower l. With the notation introduced above, the defender decision problem that maximizes the expected defender utility by adjusting the frequency variables is:

$$\begin{aligned} \max \ & \sum_{l=1}^{p} \sum_{i=1}^{n} \pi^l y_i^l(x) \left(x_i \bar{R}_i^l + (1 - x_i) \, \bar{P}_i^l \right) \\ \text{s.t.} \ & x \in \mathcal{X} \ . \end{aligned}$$

Substituting (2) above and multiplying the objective by -1 we observe that the above problem is equivalent to the minimization problem (1) by setting $\beta_i^l = e^{\lambda^l R_i^l} > 0$, $\gamma_i^l = \lambda^l (R_i^l - P_i^l) \geq 0$, $a_i^l = -\bar{P}_i^l \geq 0$ and $b_i^l = \bar{R}_i^l - \bar{P}_i^l \geq 0$.

2.2 Entropic utility defender problem

We now formulate the defender's problem with the entropic risk measure objective. The random variable of defender utilities takes the following values for each $l \in [p], \ i \in [n]$:

$$\begin{array}{ll} \bar{P}_i^l & \text{with probability} \ \ \pi^l y_i^l(x)(1 - x_i) \\ \bar{R}_i^l & \text{with probability} \ \ \pi^l y_i^l(x) x_i \ . \end{array}$$

For a random variable Y the entropic risk measure of parameter $\alpha \geq 0$ is $\alpha \ln \mathbb{E}\left[e^{\frac{Y}{\alpha}} \right]$ which penalizes values of Y that exceed the threshold parameter α. Since the defender is interested in maximizing its utility, the payoffs that should be penalized by the risk measure are the small ones. We do this by minimizing minus the utility (cost). The entropic risk objective of the cost of the defender is given by

$$\mathrm{E}_\alpha(x) := \alpha \ln \sum_{l=1}^{p} \sum_{i=1}^{n} \pi^l y_i^l(x) \left(x_i e^{-\frac{\bar{R}_i^l}{\alpha}} + (1 - x_i) \, e^{-\frac{\bar{P}_i^l}{\alpha}} \right).$$

The defender's decision problem, to minimize this entropic risk objective adjusting the frequency of coverage variables $x \in \mathcal{X}$ is expressed as follows:

$$\min_{x\in\mathcal{X}} \alpha \ln \sum_{l=1}^{p}\sum_{i=1}^{n} \pi^l y_i^l(x) \left(x_i e^{-\frac{\bar{R}_i^l}{\alpha}} + (1-x_i)\, e^{-\frac{\bar{P}_i^l}{\alpha}} \right) .$$

Define the following constants $\widetilde{P}_i^l := e^{-\frac{\bar{P}_i^l}{\alpha}}$ and $\widetilde{R}_i^l := e^{-\frac{\bar{R}_i^l}{\alpha}}$. Substituting the expression of the quantal response (2) in the problem above and noting that $\alpha \ln$ is a monotonic increasing function, we can express this problem equivalently as:

$$\min_{x\in\mathcal{X}} \quad \sum_{l=1}^{p} \pi^l \frac{\sum\limits_{i=1}^{n} \beta_i^l e^{-\gamma_i^l x_i} \left(\widetilde{P}_i^l - \left(\widetilde{P}_i^l - \widetilde{R}_i^l \right) x_i \right)}{\sum\limits_{i=1}^{n} \beta_i^l e^{-\gamma_i^l x_i}}.$$

Again, this problem is of the form of the minimization problem (1) with the same $\beta_i^l > 0$ and $\gamma_i^l \geq 0$ and with $a_i^l = \widetilde{P}_i^l > 0$ and $b_i^l = \widetilde{P}_i^l - \widetilde{R}_i^l > 0$.

The solutions x^* and $\tilde{x}$ of the example in Table 1 are obtained by solving the problems introduced in Subsections 2.1 and 2.2, respectively. Here the problems have a single adversary and the defender variables satisfy $x_1, x_2 \in [0,1]$ such that $x_1 + x_2 \leq 1$.

2.3 Piecewise linear approximations

Piecewise linear approximations of non-linear, non convex functions are an important part of the solution methods proposed. Here we set the notation used to construct piecewise linear approximations using few binary variables (a logarithm of the number of partitions), as described in [24].

Consider an univariate function $f : [l,u] \mapsto \mathbb{R}$ and a partition of the interval $[l,u]$ given by $K+1$ points $l = t_0 < t_1 < ... < t_K = u$. A piecewise linear approximation of f that matches the function at the partition points is given by $\sum_{k=0}^{K} \lambda_k f(t_k)$ with $\sum_{k=0}^{K} \lambda_k = 1$, $\lambda \geq 0$, and such that it has at most two coefficients that are non-zero and they must be consecutive (this last constraint is known as an SOS2 constraint). The work in [24] provides an efficient representation of these SOS2 constraints, which directly implies the next result.

Let $L(K) = \lceil \log_2 K \rceil$ and consider $B_K : [K] \longmapsto \{0,1\}^{L(K)}$ a bijective mapping such that for all $q \in [K-1]$, $B_K(q)$ and $B_K(q+1)$ differ in at most one component (See *reflected binary* or *Gray code* in [8]). Such a Gray code can be found quickly by the recursive algorithm of [14].

Proposition 1 *[24] Given $f : [l,u] \to \mathbb{R}$ and a partition $l = t_0 < t_1 < ... < t_K = u$ of $[l,u]$. For every $x \in [l,u]$ the piecewise linear function that equals $f(x)$ at the*

partition points is given by $\widehat{f}(x) = \sum_{k=0}^{K} \lambda_k f(t_k)$, *for a* (λ, z) *that satisfies*

$$\begin{aligned}
& x = \sum_{k=0}^{K} \lambda_k t_k \\
& \sum_{k=0}^{K} \lambda_k = 1 \\
& \sum_{p \in S_K^+(l)} \lambda_p \leqslant z_l \qquad \forall l \in [L(K)] \\
& \sum_{p \in S_K^-(l)} \lambda_p \leqslant 1 - z_l \qquad \forall l \in [L(K)] \\
& z_l \in \{0,1\} \qquad \forall l \in [L(K)] \\
& \lambda \geq 0 \ .
\end{aligned} \tag{3}$$

Here $Q_K(k) := \{k, k+1\}$ *if* $k \in [K-1]$ *and* $Q_K(K) = \{K\}$ *and for* $k \in [L(K)]$ *define:*

$$\begin{aligned}
S_K^+(k) &:= \left\{ p \in \{0, ..., K\} : \forall q \in Q_K(p), (B_K(q))_k = 1 \right\} \\
S_K^-(k) &:= \left\{ p \in \{0, ..., K\} : \forall q \in Q_K(p), (B_K(q))_k = 0 \right\} \ .
\end{aligned}$$

This formulation uses only $\lceil \log_2 K \rceil$ extra binary variables. Given a partition set $t = (t_0, \ldots, t_K)$ with $K+1$ points, we define the set of constraints that encode the piecewise linear approximation at x by:

$$LPL(t, K, x) := \left\{ \left((\lambda_k)_{k \in [K]}, (z_l)_{l \in [L(K)]} \right) \text{ satisfying (3) } \right\}.$$

We refer to this construction of a piecewise linear approximation as the Logarithmic Piecewise Linear approximation (LPL). We can therefore express the approximation of $f(x)$ by

$$\widehat{f}(x) = \sum_{k=0}^{K} \lambda_k f(t_k) \ \text{ s.t. } \ (\lambda, z) \in LPL(t, K, x) \ .$$

Remark 1 The piecewise linear function $\widehat{f}$ which equals function f at all points in a partition set t of the interval $[l, u]$ satisfies the following [22]:

1. If f is a convex function, then $\widehat{f}(x) \geq f(x)$ for all $x \in [l, u]$.
2. If f is $\mathcal{L}$-Lipschitz over $[l, u]$, then $\max_{x \in [l,u]} |\widehat{f}(x) - f(x)| \leq \frac{\mathcal{L}}{2} \max_{i \in [K-1]} |t_{i+1} - t_i|$.

3 Solution methods

In this section we present two different solution methods to solve problem (1). We begin with the observation that the numerators in each fractional term of the objective function can be considered non-negative without loss of generality. In fact, for any constant $A_l \in \mathbb{R}$ with $l \in [p]$ we have that

$$\frac{\sum_{i=1}^{n} \beta_i^l e^{-\gamma_i^l x_i} \left(a_i^l - b_i^l x_i \right)}{\sum_{i=1}^{n} \beta_i^l e^{-\gamma_i^l x_i}} = \frac{\sum_{i=1}^{n} \beta_i^l e^{-\gamma_i^l x_i} \left(A_l + a_i^l - b_i^l x_i \right)}{\sum_{i=1}^{n} \beta_i^l e^{-\gamma_i^l x_i}} - A_l \ .$$

Assuming $A_l \geq \max_{i\in[n]} \left\{b_i^l - a_i^l\right\}$ and since $x_i \in [0,1]$, we can show that function $N_i^l(x_i) = \beta_i^l e^{-\gamma_i^l x_i}\left(A_l + a_i^l - b_i^l x_i\right)$ is convex and nonnegative.

To simplify our exposition in addition to function N_i^l above we introduce $D_i^l(x_i) = \beta_i^l e^{-\gamma_i^l x_i}$, $N^l(x) = \sum_{i=1}^n N_i^l(x_i)$, and $D^l(x) = \sum_{i=1}^n D_i^l(x_i)$.

3.1 A Mixed Integer Nonlinear Reformulation (MINR)

We now use the fact that both the numerator and the denominator of these fractional component are positive to reformulate (1) as follows.

Proposition 2 *For any $A_l \geq \max_{i\in[n]} \left\{b_i^l - a_i^l\right\}$ and defining:*

$$L_l^u := \ln\left(\sum_{i=1}^n \beta_i^l e^{-\gamma_i^l}\left(A_l + a_i^l - b_i^l\right)\right) \qquad U_l^u := \ln\left(\sum_{i=1}^n \beta_i^l \left(A_l + a_i^l\right)\right)$$
$$L_l^v := \ln\left(\sum_{i=1}^n \beta_i^l e^{-\gamma_i^l}\right) \qquad U_l^v := \ln\left(\sum_{i=1}^n \beta_i^l\right),$$

problem (1) *is equivalent to*

$$\begin{aligned}
\min_{x,u,v}\ & \sum_{l=1}^p \pi^l e^{u_l - v_l} \\
\text{s.t. }\ & x \in \mathcal{X} \\
& -e^{u_l} + \sum_{i=1}^n \beta_i^l e^{-\gamma_i^l x_i}\left(A_l + a_i^l - b_i^l x_i\right) \leq 0 \qquad \forall l \in [p] \\
& e^{v_l} - \sum_{i=1}^n \beta_i^l e^{-\gamma_i^l x_i} \leq 0 \qquad \forall l \in [p] \\
& L_l^u \leq u_l \leq U_l^u \qquad \forall l \in [p] \\
& L_l^v \leq v_l \leq U_l^v \qquad \forall l \in [p]
\end{aligned} \tag{4}$$

Proof First, from the observation above we can rewrite (1) as follows:

$$\min_{x\in\mathcal{X}} \sum_{l=1}^p \pi^l \left(\frac{\sum_{i=1}^n \beta_i^l e^{-\gamma_i^l x_i}\left(A_l + a_i^l - b_i^l x_i\right)}{\sum_{i=1}^n \beta_i^l e^{-\gamma_i^l x_i}} - A_l\right)$$

For each $l \in [p]$ introduce variables $(u_l, v_l) \in \mathbb{R}^2$. Since the numerator and denominator of each fraction are nonnegative, we have that this last problem can be rewritten as follows:

$$\begin{aligned}
\min_{u,v}\ & \sum_{l=1}^p \pi^l e^{u_l - v_l} - \sum_{l=1}^p \pi^l A_l \\
\text{s.t. }\ & e^{u_l} \geq \sum_{i=1}^n \beta_i^l e^{-\gamma_i^l x_i}\left(A_l + a_i^l - b_i^l x_i\right) \qquad \forall l \in [p] \\
& e^{v_l} \leq \sum_{i=1}^n \beta_i^l e^{-\gamma_i^l x_i} \qquad \forall l \in [p]\ .
\end{aligned}$$

The term $-\sum_{l=1}^{p} \pi^l A_l$ is constant. The range constraints on variables u_l and v_l are obtained by maximizing and minimizing the bounds on e^{u_l} and e^{v_l}. The facts that $A_l \geq \max_{i\in[n]}\{b_i^l - a_i^l\}$, $\gamma_i^l \geq 0$ and $b_i^l \geq 0$ imply that both these bounds are decreasing functions of x_i which obtain its maximum value for $x_i = 0$ and minimum value for $x_i = 1$. □

Given the choice of A_l, we have that the sources of non-convexity of problem (4) are the functions $u_l \to -e^{u_l}$ indexed by $l \in [p]$ in the second set of constraints and $x_i \to -e^{-\gamma_i^l x_i}$ for every $i \in [n], l \in [p]$ in the third set of constraints. This motivates the use of piecewise linear functions to approximate the problem. The LPL formulation is used below to construct piecewise linear approximations of the non-convex portions of the constraints. The range constraints on variables inform where this approximation should be done.

For each target $i \in [n]$, consider the partition t^i of $[0, 1]$ on $K + 1$ points (i.e. $0 = t_0^i < t_1^i < ... < t_K^i = 1$). For each follower $l \in [p]$, consider the partition τ^l of $[L_l^u, U_l^u]$ on $K + 1$ points (i.e. $L_l^u = \tau_0^l < \tau_1^l < ... < \tau_K^l = U_l^u$). Using these partitions we construct the following mixed integer convex optimization problem:

$$\min_{\substack{x,\,u,\,v,\,\rho,\,\vartheta\\ \theta,\,\lambda,\,z,\,\xi,\,y}} \quad \sum_{l=1}^{p} \pi^l \rho_l \tag{5}$$

$$\text{s.t.} \quad x \in \mathcal{X} \tag{6}$$

$$\rho_l \geq e^{u_l - v_l} \qquad \forall l \in [p] \tag{7}$$

$$\sum_{i=1}^{n} \theta_l^i \leq \sum_{k=0}^{K} \xi_k^l e^{\tau_k^l} \qquad \forall l \in [p] \tag{8}$$

$$\theta_l^i \geq \beta_i^l e^{-\gamma_i^l x_i} \left(A^l + a_i^l - b_i^l x_i\right) \qquad \forall l \in [p], i \in [n] \tag{9}$$

$$\vartheta_l \leq \sum_{i=1}^{n} \beta_i^l \sum_{k=0}^{K} \lambda_k^i e^{-\gamma_i^l t_k^i} \qquad \forall l \in [p] \tag{10}$$

$$\vartheta_l \geq e^{v_l} \qquad \forall l \in [p] \tag{11}$$

$$L_l^u \leq u_l \leq U_l^u \qquad \forall l \in [p] \tag{12}$$

$$L_l^v \leq v_l \leq U_l^v \qquad \forall l \in [p] \tag{13}$$

$$e^{L_l^u - U_l^v} \leq \rho_l \leq e^{U_l^u - L_l^v} \qquad \forall l \in [p] \tag{14}$$

$$e^{L_l^v} \leq \vartheta_l \leq e^{U_l^v} \qquad \forall l \in [p] \tag{15}$$

$$\left(\lambda^i, z^i\right) \in LPL\left(t^i, K, x_i\right) \qquad \forall i \in [n] \tag{16}$$

$$\left(\xi^l, y^l\right) \in LPL\left(\tau^l, K, u_l\right) \qquad \forall l \in [p] \tag{17}$$

This approximate problem has integer variables z and y defined in the LPL constraints and convex constraints in (7), (9) and (11). The following result shows that the optimal solution to this problem provides a good solution to (4).

Proposition 3 *Consider uniform partitions t and τ with $K + 1$ points in the definition of problem (5-17). Let $\widehat{\kappa}$ be the optimal solution value of the approximate*

problem (5-17) and κ the optimal solution value of the original problem (1)*, then* $0 \leq \kappa - \widehat{\kappa} \leq O(1/K)$*. Furthermore,* $\overline{x} \in \mathcal{X}$ *part of optimal solution to (5-17) is feasible for* (1) *with objective* $\kappa(\overline{x})$ *such that* $|\kappa(\overline{x}) - \kappa| \leq O(1/K)$*.*

Proof We begin showing that $\widehat{\kappa} \leq \kappa$ by using (x^*, u^*, v^*) an optimal solution for (4) (since by Proposition 2 it is equivalent to (1)) to construct a feasible point in (5-17). Given x^* and u_l^* the LPL constraints define unique variables λ^*, z^* and ξ_l^*, y_l^* to satisfy these constraints. Setting $\rho_l^* := e^{u_l^* - v_l^*}$, $\theta_l^{i*} := N_i^l(x_i^*)$ and $\vartheta_l^* := e^{v_l^*}$ we have that $(x^*, u^*, v^*, \rho^*, \vartheta^*, \theta^*, \lambda^*, z^*, \xi^*, y^*)$ is feasible for (5-17). Checking the constraints uses the inequalities that (x^*, u^*, v^*) satisfies from problem (4) and Remark 1.

For the second part we begin with $\left(\overline{x}, \overline{u}, \overline{v}, \overline{\rho}, \overline{\vartheta}, \overline{\theta}, \overline{\lambda}, \overline{z}, \overline{\xi}, \overline{y}\right)$ the optimal solution to (5-17) and show that a slight change is feasible for (4). Notice that $\overline{x} \in \mathcal{X}$, therefore feasible for (1). By inspection we can verify this optimal solution satisfies:

$$\overline{\rho}_l = e^{\overline{u}_l - \overline{v}_l} \qquad \widehat{e^{\overline{u}_l}} = N^l(\overline{x}) \qquad e^{\overline{v}_l} = \widehat{D^l(\overline{x})} \ . \tag{18}$$

However, feasible solutions to (4) satisfy that $e^{u_l} \geq N^l(x)$ and $e^{v_l} \leq D^l(x)$. Recall $\widehat{f}$ is the piecewise linear approximation of f. From Remark 1 we have that $D^l(x) \leq \widehat{D^l(x)} \leq D^l(x) + \varepsilon_1$ and that $e^{u_l} \leq \widehat{e^{u_l}} \leq e^{u_l} + \varepsilon_2$. The values ε_1 and ε_2 are of the form $\mathcal{L}C/(2K)$ which is $O(1/K)$. Here $\mathcal{L}$ is a constant that depends on the function being approximated and C/K denotes the interval width in the uniform partition. Combining these bounds with the last two equalities in (18), we can define u_l' and v_l' such that

$$e^{u_l'} := e^{\overline{u}_l} + \varepsilon_2 \geq N^l(\overline{x}) \qquad e^{v_l'} := e^{\overline{v}_l} - \varepsilon_1 \leq D^l(\overline{x}) \ . \tag{19}$$

The solution $\left(\overline{x}, u', v'\right)$ is then feasible for (4), which means

$$\kappa \leq \sum_{l=1}^{p} \pi^l e^{u_l' - v_l'} = \sum_{l=1}^{p} \pi^l \frac{e^{\overline{u}_l} + \varepsilon_2}{e^{\overline{v}_l} - \varepsilon_1} \ .$$

From the first part we obtain that $0 \leq \kappa - \widehat{\kappa}$. The first equation in (18) implies that $\widehat{\kappa} = \sum_{l=1}^{p} \pi^l e^{\overline{u}_l - \overline{v}_l}$. Combining this with the last expression we have

$$0 \leq \kappa - \widehat{\kappa} \leq \sum_{l=1}^{p} \pi^l \left(\frac{e^{\overline{u}_l} + \varepsilon_2}{e^{\overline{v}_l} - \varepsilon_1} - \frac{e^{\overline{u}_l}}{e^{\overline{v}_l}} \right) = \sum_{l=1}^{p} \pi^l \left(\frac{\varepsilon_2 e^{\overline{v}_l} + \varepsilon_1 e^{\overline{u}_l}}{e^{\overline{v}_l}\left(e^{\overline{v}_l} - \varepsilon_1\right)} \right) \ .$$

From Remark 1 and (18) we have that $N^l(\overline{x}) \geq e^{\overline{u}_l}$ and $e^{\overline{v}_l} \geq D^l(\overline{x})$. Defining $N^+ := \max_{l \in [p], x \in \mathcal{X}} N^l(x)$, $D^+ := \max_{l \in [p], x \in \mathcal{X}} D^l(x)$, $D^- := \min_{l \in [p], x \in \mathcal{X}} D^l(x)$, and $\epsilon = \max\{\epsilon_1, \epsilon_2\}$ we obtain the following bound that gives the result since $\epsilon = O(1/K)$

$$0 \leq \kappa - \widehat{\kappa} \leq \epsilon \ \frac{N^+ + D^+ + \varepsilon_1}{D^-\left(D^- - \varepsilon_1\right)} \ .$$

Now we show that $|\kappa - \kappa(\overline{x})|$ is $O(1/K)$. From the second part we have that $\overline{x}$ is feasible for (1) and $\kappa \geq \widehat{\kappa}$. This, and the inequalities in (19) imply

$$\kappa \geq \widehat{\kappa} = \sum_{l=1}^{p} \pi^l \frac{e^{\overline{u}_l}}{e^{\overline{v}_l}} = \sum_{l=1}^{p} \pi^l \frac{N^l(\overline{x}) - \varepsilon_2}{D^l(\overline{x}) + \varepsilon_1} \ .$$

Since $\kappa(\overline{x}) = \sum_{l=1}^{p} \pi^l \frac{N^l(\overline{x})}{D^l(\overline{x})}$, we have, similarly to the previous derivation, that

$$0 \leq \kappa(\overline{x}) - \kappa \leq \sum_{l=1}^{p} \pi^l \left(\frac{N^l(\overline{x})}{D^l(\overline{x})} - \frac{N^l(\overline{x}) - \varepsilon_2}{D^l(\overline{x}) + \varepsilon_1} \right) \leq \epsilon \, \frac{N^+ + D^+}{D^- \, (D^- + \varepsilon_1)}. \qquad \square$$

Solving problem (5-17) is challenging as it is a problem with convex constraints and integer variables. To avoid the non-linearity, we approximate the convex portions of the constraint functions exploiting the fact that a convex function is the upper envelope of the linear support functions at every point. In particular we replace the convex non-linear terms of the functions $e^{u_l - v_l}$, given $l \in [p]$, e^{v_l}, and $N_i^l(x_i) = \beta_i^l e^{-\gamma_i^l x_i} \left(A_l + a_i^l - b_i^l x_i \right)$ with their first order Taylor expansions. This modifies only constraints (7), (9), and (11) giving the mixed integer linear optimization problem (with infinitely many constraints):

$$\begin{array}{lll} \min\limits_{\substack{x,\, u,\, v,\, \rho,\, \vartheta \\ \theta,\, \lambda,\, z,\, \xi,\, y}} & \sum\limits_{l=1}^{p} \pi^l \rho_l & \\ \text{s.t.} & (6), (8), (10), (12), (13), (14), (15), (16), (17) & \\ & \rho_l \geq e^{\hat{u}_l - \hat{v}_l} \left(1 + u_l - v_l - \hat{u}_l + \hat{v}_l \right) & \forall (\hat{u}_l, \hat{v}_l) \\ & & l \in [p] \\ & \theta_l^i \geq N_i^l \left(\hat{x}_i \right) + \left(N_i^l \right)' \left(\hat{x}_i \right) \left(x_i - \hat{x}_i \right) & \forall \hat{x}_i \\ & & \forall l \in [p], i \in [n] \\ & \vartheta_l \geq e^{\hat{v}_l} \left(1 + v_l - \hat{v}_l \right) & \forall \hat{v}_l \quad l \in [p] \; . \end{array} \tag{20}$$

To tackle the infinitely many constraints in the above problem, we will generate them as we need them with a cutting plane procedure. We set up the problem with an initial set of linear support functions. Let $\mathcal{U}_l^{u,v}$ be the set of points used to build linear support function of $(u_l, v_l) \to e^{u_l - v_l}$, given $l \in [p]$. Similarly let $\mathcal{U}_l^v$ and $\mathcal{U}_{li}^x$ be the set of points used to generate linear support functions of $v_l \to e^{v_l}$ and N_i^l, respectively. The tractable optimization problem is (20) replacing the last three constraints with the following.

$$\begin{array}{ll} \rho_l \geq e^{\hat{u}_l - \hat{v}_l} \left(1 + u_l - v_l - \hat{u}_l + \hat{v}_l \right) & \forall (\hat{u}_l, \hat{v}_l) \in \mathcal{U}_l^{u,v} \\ & l \in [p] \\ \theta_l^i \geq N_i^l \left(\hat{x}_i \right) + \left(N_i^l \right)' \left(\hat{x}_i \right) \left(x_i - \hat{x}_i \right) & \forall \hat{x}_i \in \mathcal{U}_{li}^x \\ & \forall l \in [p], i \in [n] \\ \vartheta_l \geq e^{\hat{v}_l} \left(1 + v_l - \hat{v}_l \right) & \forall \hat{v}_l \in \mathcal{U}_l^v, l \in [p] \; . \end{array}$$

3.2 Multidimensional cell approximation with $(n+p)\log_2 K$ binaries (CELL)

We now present a generic method to approximate nonseparable functions using linear constraints and variables, in the spirit of [19].

We transform our problem (1) into the following equivalent form:

$$\min_{x \in \mathcal{X}, \rho} \left\{ \sum_{l=1}^{p} \pi^l \rho_l : \sum_{i=1}^{n} \left(N_i^l \left(x_i \right) - \rho_l D_i^l \left(x_i \right) \right) \leq 0 \quad , \forall l \in [p] \right\} \tag{21}$$

This problem is in general not convex because of the products $\rho_l D_i^l(x_i)$. Similar to the previous model, we added and subtracted $A_l \geq \max_{i\in[n]}\{bi^l - a_i^l\}$ to the numerator of (1) so that $N_i^l(x_i)$ is convex and non-negative.

To tackle this non-convexity, we take advantage of the partial separability in the constraints of (21) to efficiently approximate the products $\rho_l D_i^l(x_i)$ with a relatively small number of binary variables. The following proposition presents this piecewise linear approximation on a given homogeneous grid, which is a variant of the method referred to as the optimistic MILP model in [19].

Proposition 4 *Consider a ground set $\mathcal{G} := \left\{x \in \mathbb{R}^I : l \leq x \leq u\right\}$ and a set of J functions $f_j : \mathcal{G} \to \mathbb{R}$, each one of them $\mathcal{L}_j$-Lipschitz. Also consider a discretization of $\mathcal{G}$ in each dimension: $l_i = t_0^i \leq t_1^i \leq ... \leq t_K^i = u_i$, where $t_{k_i}^i = l_i + \frac{k_i}{K}(u_i - l_i)$ for every $k_i \in \{0, ..., K\}$. The following formulation gives an $\mathcal{L}_j||u-l||_1/K$ approximation $\bar{f}_j$ for every function f_j on $\mathcal{G}$:*

$$
\begin{aligned}
\bar{f}_j(x) = \min_{\mu,\lambda,z} \quad & \sum_{k\in\{0,\dots,K\}^I} \mu_k \cdot f_j\left(t_{k_1}^1, ..., t_{k_I}^I\right) & \\
\text{s.t.} \quad & \left(\lambda^i, z^i\right) \in LPL\left(t^i, K, x_i\right) & \forall i \in [I] \\
& \mu_k \leq \lambda_{k_i}^i & \forall k \in \{0, ..., K\}^I \\
& & \forall i \in [I] \\
& \sum_{k\in\{0,\dots,K\}^I} \mu_k = 1 & \\
& \sum_{k\in\{0,\dots,K\}^I} \mu_k t_{k_i}^i = x_i & \forall i \in [I] \\
& \mu \geq 0 &
\end{aligned}
\tag{22}
$$

Proof Let us consider some $j \in [J]$. By definition of $\bar{f}_j(\cdot)$, for any $x \in \mathcal{G}$ there exists some tuple (μ, λ, z) satisfying (22) such that

$$
\begin{aligned}
\Delta_j(x) := \left|f_j(x) - \bar{f}_j(x)\right| &= \left| f_j(x) - \sum_{k\in\{0\dots K\}^I} \mu_k \cdot f_j\left(t_{k_1}^1, ..., t_{k_I}^I\right) \right| \\
&= \left| \sum_{k\in\{0\dots K\}^I} \mu_k \cdot \left[f_j(x) - f_j\left(t_{k_1}^1, ..., t_{k_I}^I\right) \right] \right| \\
&\leq \sum_{k\in\{0\dots K\}^I} \mu_{k_1,\dots,k_I} \cdot \left| f_j(x) - f_j\left(t_{k_1}^1, ..., t_{k_I}^I\right) \right| \ .
\end{aligned}
$$

Here the second equality is due to $||\mu||_1 = 1$ and the inequality because of the convexity of $|\cdot|$. Next, because we have $\left(\lambda^i, z^i\right) \in LPL\left(t^i, K, x_i\right)$ for any $i \in [I]$, there is an index $k_i^x \in \{0, ..., K-1\}$ such that $t_{k_i^x}^i \leq x_i \leq t_{k_i^x+1}^i$ and the only possible nonzero values of λ^i are $\lambda_{k_i^x}^i$ and $\lambda_{k_i^x+1}^i$. In consequence, the precedence constraints (second set of contraints in (22)) enforce that the only possible nonzero

values of μ are the $\mu_{k_1,...,k_I}$ with $k_i \in \{k_i^x, k_i^x + 1\}$ for every $i \in [I]$. We then obtain:

$$\begin{aligned}\Delta_j(x) &\leq \sum_{k_1=k_1^x}^{k_1^x+1} ... \sum_{k_I=k_I^x}^{k_I^x+1} \mu_{k_1,...,k_I} \cdot \left| f_j(x) - f_j\left(t^1_{k_1}, ..., t^I_{k_I}\right)\right| \\ &\leq \max_{k_i \in \left\{k_i^x, k_i^x+1\right\}, i\in[I]} \left| f_j(x) - f_j\left(t^1_{k_1}, ..., t^I_{k_I}\right)\right| \|\mu\|_1 \\ &\leq \max_{k_i \in \left\{k_i^x, k_i^x+1\right\}, i\in[I]} \mathcal{L}_j \left\| x - \left(t^1_{k_1}, ..., t^I_{k_I}\right)\right\|_1 = \mathcal{L}_j \sum_{i=1}^{I} \max_{k_i \in \left\{k_i^x, k_i^x+1\right\}} \left| x_i - t^i_{k_i}\right|\end{aligned}$$

Where the $\mathcal{L}_j$-Lipschitz assumption and $\|\mu\|_1 = 1$ are used. Define $\mathcal{G}(x)$ as the *cell* of the discretization of $\mathcal{G}$ that contains x, i.e.

$$\mathcal{G}(x) := \left\{x' \in \mathcal{G} : t^i_{k_i^x} \leq x'_i \leq t^i_{k_i^x+1}, \forall i \in [I]\right\}.$$

Given that $x \in \mathcal{G}(x)$ we have that:

$$\begin{aligned}\Delta_j(x) &\leq \max_{x' \in \mathcal{G}(x)} \mathcal{L}_j \sum_{i=1}^{I} \max_{k_i \in \left\{k_i^x, k_i^x+1\right\}} \left| x'_i - t^i_{k_i}\right| \\ &= \mathcal{L}_j \sum_{i=1}^{I} \max_{k_i \in \left\{k_i^x, k_i^x+1\right\}} \max_{x'_i \in \left[t^i_{k_i^x}, t^i_{k_i^x+1}\right]} \left| x'_i - t^i_{k_i}\right| \\ &= \mathcal{L}_j \sum_{i=1}^{I} \left| t^i_{k_i^x+1} - t^i_{k_i^x}\right| = \frac{\mathcal{L}_j}{K} \sum_{i=1}^{I} |u_i - l_i| = \frac{\mathcal{L}_j}{K} ||u - l||_1 \ . \qquad \square\end{aligned}$$

This result shows that the maximum distance between $\hat{f}_j$ and f_j is $O(1/K)$. Also, the size of the optimization problem that approximates function f_j does not depend on the number of functions to approximate J. The optimization problem uses $L(K)I$ binary variables, $O\left(K^I\right)$ continuous variables and $O\left(IK^I\right)$ constraints. A direct consequence is the piecewise linear cell formulation of an optimization problem, stated below.

Proposition 5 *Given an optimization problem*

$$\begin{aligned}&\min_{x \in \mathcal{X}} f(x) \\ &\text{s.t. } g_j(x) \leq b_j \ \forall j \in \{1, ..., J\},\end{aligned}$$

its cell-approximation is given by the following MIP

$$\begin{aligned}\min_{x\in\mathcal{X},\mu,\lambda,z} \quad & \sum_{k\in\{0,...,K\}^I} \mu_k \cdot f\left(t^1_{k_1}, ..., t^I_{k_I}\right) & & \\ \text{s.t.} \quad & \sum_{k\in\{0,...,K\}^I} \mu_k \cdot g_j\left(t^1_{k_1}, ..., t^I_{k_I}\right) \leq b_j \ \forall j \in [J] & & \\ & \left(\lambda^i, z^i\right) \in LPL\left(t^i, K, x_i\right) & \forall i \in [I] & \\ & \mu_k \leq \lambda^i_{k_i} & \forall k \in \{0, ..., K\}^I & \quad (23) \\ & & \forall i \in [I] & \\ & \sum_{k\in\{0,...,K\}^I} \mu_k = 1 & & \\ & \sum_{k\in\{0,...,K\}^I} \mu_k t^i_{k_i} = x_i & \forall i \in [I] & \\ & \mu \geq 0 & &\end{aligned}$$

This formulation takes advantage of the fact that we only need to determine once to which cell x belongs and use this to approximate every function in the problem. Therefore the number of binary variables does not depend on the number of functions to approximate. We now show that using the cell discretization, the solution we obtain is an $O(1/K)$-optimal solution for our original SSG problem.

Proposition 6 *Consider a discretization of the range of variables x_i and ρ_l into K subintervals with homogeneous partitions $t^i = \left(t^i_0 \dots t^i_K\right)$ and $\tau^l = \left(\tau^l_0 \dots \tau^l_K\right)$. Let $\widehat{\kappa}$ be the optimal solution value of problem (24), $\overline{x}$ part of its optimal solution. Let also $\kappa(\overline{x})$ the objective function value and κ the optimal solution value of problem (1). Then $|\widehat{\kappa} - \kappa|$ and $|\kappa(\overline{x}) - \kappa|$ are $O(1/K)$.*

$$
\begin{aligned}
\min_{x,\rho,\lambda,y,\xi,z,\mu} \quad & \sum_{l=1}^{p} \pi^l \rho_l \\
\text{s.t.} \quad & x \in \mathcal{X} \\
& \sum_{i=1}^{n} \sum_{k=0}^{K} \lambda^i_k N^l_i\left(t^i_k\right) \\
& \qquad - \sum_{i=1}^{n} \sum_{k_l=0}^{K} \sum_{k_i=0}^{K} \mu^{l,i}_{k_l,k_i} \tau^l_{k_l} D^l_i\left(t^i_{k_i}\right) \leq 0 \;\; \forall l \in [p] \\
& \left(\lambda^i, z^i\right) \in LPL\left(t^i, K, x_i\right) && \forall i \in [n] \\
& \left(\xi^l, y^l\right) \in LPL\left(\tau^l, K, \rho_l\right) && \forall l \in [p] \\
& 0 \leq \mu^{l,i}_{k_l,k_i} \leq \xi^l_{k_l} && \forall k_l, k_i \in \{0, ..., K\} \\
& && \forall l, i \in [p] \\
& 0 \leq \mu^{l,i}_{k_l,k_i} \leq \lambda^i_{k_i} && \forall k_l, k_i \in \{0, ..., K\} \\
& && \forall l, i \in [p] \\
& \sum_{k_l=0}^{K} \sum_{k_i=0}^{K} \mu^{l,i}_{k_l,k_i} = 1 && \forall l \in [p], \forall i \in [n] \\
& \sum_{k_l=0}^{K} \sum_{k_i=0}^{K} \mu^{l,i}_{k_l,k_i} t^i_{k_i} = x_i && \forall i \in [n] \\
& \sum_{k_l=0}^{K} \sum_{k_i=0}^{K} \mu^{l,i}_{k_l,k_i} \tau^l_{k_l} = \rho_l && \forall l \in [p]
\end{aligned}
\tag{24}
$$

Proof First, for any $x \in \mathcal{X}$ and $\rho_l \in \mathbb{R}, l \in [p]$, we have from Proposition 4 that

$$
-\epsilon_l \leq N_l(x) - \rho_l D_l(x) - \left[\bar{N}_l(x) - \bar{D}_l\left(x, \rho_l\right)\right] \leq \epsilon_l \ ,
$$

for some $\epsilon_l > 0$ (that is $O(1/K)$). Where $\bar{f}$ is the approximation of f. Defining $\rho^*_l(x) := \frac{N_l(x)}{D_l(x)}$ and using $D_l(x) > 0$, we obtain:

$$
\frac{\bar{N}_l(x) - \bar{D}_l\left(x, \rho_l\right) - \epsilon_l}{D_l(x)} + \rho_l \leqslant \rho^*_l(x) \leq \frac{\bar{N}_l(x) - \bar{D}_l\left(x, \rho_l\right) + \epsilon_l}{D_l(x)} + \rho_l. \tag{25}
$$

Consider $\left(\overline{x}, \overline{\rho}, \overline{\lambda}, \overline{y}, \overline{\xi}, \overline{z}, \overline{\mu}\right)$ the optimal solution of (24). From these constraints we have that $\bar{N}_l\left(\overline{x}\right) - \bar{D}_l\left(\overline{x}, \overline{\rho}\right) \leq 0$. Using the right inequality in (25) at $\overline{x}$, $\overline{\rho}$ gives

$$\kappa\left(\overline{x}\right) = \sum_{l=1}^{p} \pi^l \rho_l^*\left(\overline{x}\right) \leq \sum_{l=1}^{p} \pi^l \left(\frac{\epsilon_l}{D_l\left(\overline{x}\right)} + \bar{\rho}_l\right) \tag{26}$$

$$= \sum_{l=1}^{p} \frac{\pi^l \epsilon_l}{D_l\left(\overline{x}\right)} + \widehat{\kappa}$$

$$\leq \sum_{l=1}^{p} \frac{\pi^l \epsilon_l}{D_l\left(\overline{x}\right)} + \widehat{\kappa}\left(x^*\right) \tag{27}$$

Here we use that $\overline{x}$, $\overline{\rho}$ are optimal for (24) and denote $\widehat{\kappa}(x^*)$ the objective value of (24) on solution x^*.

Second, consider a function $f : \mathbb{R}^n \to \mathbb{R}$ and its cell-approximation $\bar{f}$. Notice that if the function $t \to f\left(x_1, ..., x_{i-1}, t, x_{i+1}, ..., x_n\right)$ is nondecreasing, then so is the function $t \to \bar{f}\left(x_1, ..., x_{i-1}, t, x_{i+1}, ..., x_n\right)$. Since $\rho \to -\rho D_l(x)$ is decreasing then so is $\rho \to -\bar{D}_l(x, \rho)$. This means that we can find $\bar{\rho}_l(x)$ such that $\bar{N}_l(x) - \bar{D}_l\left(x, \bar{\rho}_l(x)\right) = 0$. Consider now x^* the optimal solution to (1) Taking the left inequality of (25) x^* and $\bar{\rho}_l\left(x^*\right)$ we obtain:

$$\widehat{\kappa}(x^*) = \sum_{l=1}^{p} \pi^l \bar{\rho}_l\left(x^*\right) \leq \sum_{l=1}^{p} \pi^l \left(\rho_l^*\left(x^*\right) + \frac{\epsilon_l}{D_l\left(x^*\right)}\right)$$

$$\leq \kappa + \sum_{l=1}^{p} \frac{\pi^l \epsilon_l}{D_l\left(x^*\right)} \tag{28}$$

Adding (27) and (28) together, and defining $D^- = \min_{l \in [p], x \in \mathcal{X}} D_l(x)$ and $\epsilon = \max_{l \in [p]} \epsilon_l$, we get:

$$0 \leq \kappa\left(\overline{x}\right) - \kappa \leq \sum_{l=1}^{p} \pi^l \epsilon_l \left(\frac{1}{D_l\left(\bar{x}\right)} + \frac{1}{D_l\left(x^*\right)}\right) \leq \frac{2\epsilon}{D^-} \ .$$

To finish, we now prove that $|\kappa - \widehat{\kappa}| = O(1/K)$. From (26) and by optimality of x^* we obtain:

$$\kappa - \widehat{\kappa} \leq \kappa(\overline{x}) - \widehat{\kappa} \leq \sum_{l=1}^{p} \frac{\pi^l \epsilon_l}{D_l\left(\bar{x}\right)} \leq \frac{\epsilon}{D^-} \tag{29}$$

Further, from (28) and by optimality of $\bar{x}$ we obtain:

$$\widehat{\kappa} - \kappa \leq \widehat{\kappa}(x^*) - \kappa \leq \sum_{l=1}^{p} \frac{\pi^l \epsilon_l}{D_l\left(x^*\right)} \leq \frac{\epsilon}{D^-} \tag{30}$$

finishing the proof. □

Notice that the approach is valid for any fractional programming problem having separable numerators and denominators. In our case, however, using the A_l trick from the last subsection makes all the numerators convex. This implies that we are not forced to use an a priori cell approximation for them as depicted

in the second constraint of (24). In consequence we can use again a cutting plane approach by adding additional variables θ_l and replacing the linearized constraints of $N_i^l(x_i)$ in (24) by the following:

$$\begin{aligned}
\sum_{i=1}^{n} \theta_l^i \leq \sum_{i=1}^{n} \sum_{k_l=0}^{K} \sum_{k_i=0}^{K} \mu_{k_l,k_i}^{l,i} \tau_{k_l}^l D_i^l \left(t_{k_i}^i\right) \qquad & \forall l \in [p] \\
\theta_l^i \geq N_i^l(\hat{x}_i) + \left(N_i^l\right)'(\hat{x}_i)(x_i - \hat{x}_i) \qquad & \forall \hat{x}_i, \qquad (31) \\
& \forall l \in [p], \forall i \in [n]
\end{aligned}$$

The same approximation bound is achieved with smaller tolerances. We can also consider the bounds for the objective ρ_l and the new variables θ_l

$$\begin{aligned}
e^{L_l^u - U_l^v} \leq \rho_l \leq e^{U_l^u - L_l^v} \qquad & ,\forall l \in [p] \\
e^{L_l^u} \leq \theta_l \leq e^{U_l^u} \qquad & ,\forall l \in [p]
\end{aligned}$$

Last but not least, not using an LPL approximation for the numerators N^l ensures that $\hat{\kappa}$ is a genuine lower bound for κ by using a proof similar to the last Proposition.

3.3 A cutting plane approach

The main problem with the cell-approximation (22) is the number of precedence constraints (the second set of constraints in (22)) and the dimension $\{0, ..., K\}^I$ of the variable μ. To bypass this issue, we propose the following cutting plane approach for the generic optimization problem (23):

Proposition 7 *Given fixed variables (x, λ, z) for problem (23), we consider the μ subproblem of (23) (i.e. the problem of optimizing only with respect to μ). The dual of the μ subproblem in (23) is:*

$$\begin{aligned}
\max_{p,c,d,s} \quad & -\sum_{i=1}^{I} \sum_{k \in \{0,...,K\}^I} p_{ki} \lambda_{k_i}^i + c + \sum_{i=1}^{I} d_i x_i - \sum_{j=1}^{J} s_j b_j \\
\text{s.t.} \quad & -\sum_{i=1}^{I} p_{ki} \lambda_{k_i}^i + c + \sum_{i=1}^{I} d_i t_{k_i}^i - \sum_{j=1}^{J} s_j g_j \left(t_{k_1}^1, ..., t_{k_I}^I\right) \\
& \qquad \leq f\left(t_{k_1}^1, ..., t_{k_I}^I\right) \quad \forall k \in \{0, ..., K\}^I \\
& p, s \geq 0
\end{aligned}$$

The cuts added to the relaxed problem are the following

$$\eta \geq -\sum_{i=1}^{I} \sum_{k \in \{0,...,K\}^I} \hat{p}_{ki} \lambda_{k_i}^i + \hat{c} + \sum_{i=1}^{I} \hat{d}_i x_i - \sum_{j=1}^{J} \hat{s}_j b_j \qquad (32)$$

$$0 \geq -\sum_{i=1}^{I} \sum_{k \in \{0,...,K\}^I} \hat{p}_{ki} \lambda_{k_i}^i + \hat{c} + \sum_{i=1}^{I} \hat{d}_i x_i - \sum_{j=1}^{J} \hat{s}_j b_j \qquad (33)$$

Note that given a feasible solution $\left(\hat{x}, \hat{\lambda}, \hat{z}\right)$ for (22), the variables $\hat{\lambda}$ are mostly zero except for at most $2I$ of them, meaning that we can fix to zero all the corresponding variables p. This suggests a Benders decomposition approach [2] to solve our cell-approximation problem (24). We begin with the following *master problem*

$$\begin{aligned}
\min_{x,\rho,\theta,\lambda,y,\xi,z} \quad & \sum_{l=1}^{p} \pi^l \rho_l \\
\text{s.t.} \quad & x \in \mathcal{X} \\
& \left(\lambda^i, z^i\right) \in LPL\left(t^i, K, x_i\right) \ \forall i \in [n] \\
& \left(\xi^l, y^l\right) \in LPL\left(\tau^l, K, \rho_l\right) \ \forall l \in [p] \\
& e^{L_l^u - U_l^v} \leq \rho_l \leq e^{U_l^u - L_l^v} \quad \forall l \in [p]
\end{aligned}$$

and add the cutting planes described in the following proposition as we need them:

Proposition 8 *When solving problem* (24) *with a cut generation strategy, if the current incumbent $\hat{x}$ of the master problem violates a linear support function constraint modeled by θ_l^i,* (31)*, then we add the following cut to the master problem:*

$$\theta_l^i \geq N_i^l\left(\hat{x}_i\right) + \left(N_i^l\right)'\left(\hat{x}_i\right)\left(x_i - \hat{x}_i\right)$$

If the current incumbent $\left(\hat{x}, \hat{\rho}, \hat{\theta}, \hat{\lambda}, \hat{\xi}\right)$ of the master problem makes the subproblem in μ infeasible, the Benders cut to add to the master problem are:

$$\begin{aligned}
&\sum_{l=1}^{p}\sum_{i=1}^{n}\sum_{k_i=0}^{K}\sum_{k_l=0}^{K}\left(\hat{r}_{k_l k_i}^{li}\xi_{k_l}^l + \hat{s}_{k_l k_i}^{li}\lambda_{k_i}^i\right) \\
&-\sum_{l=1}^{p}\hat{q}_l\sum_{i=1}^{n}\theta_l^i - \sum_{l=1}^{p}\sum_{i=1}^{n}\left(\hat{v}_{li}x_i + \hat{w}_{li}\rho_l\right) \geq \sum_{l=1}^{p}\sum_{i=1}^{n}\hat{u}_{li}
\end{aligned}$$

where $(\hat{q}, \hat{r}, \hat{s}, \hat{u}, \hat{v}, \hat{w})$ is an optimal ray of the dual of the subproblem in μ.

Notice that the dual of the subproblem in μ of formulation (24) is in fact separable in p smaller problems:

$$\begin{aligned}
\sum_{l=1}^{p} \max_{q_l, r^l, s^l, u_l, v_l, w_l} \quad & q_l\sum_{i=1}^{n}\theta_l^i - \sum_{i=1}^{n}\sum_{k_i=0}^{K}\sum_{k_l=0}^{K}\left(r_{k_l k_i}^{li}\hat{\xi}_{k_l}^l + s_{k_l k_i}^{li}\hat{\lambda}_{k_i}^i\right) \\
& + \sum_{i=1}^{n}\left(u_{li} + v_{li}\hat{x}_i + w_{li}\hat{\rho}_l\right) && (34) \\
\text{s.t.:} \quad & q_l\tau_{k_l}^l D_i^l\left(t_{k_i}^i\right) - r_{k_l k_i}^{li} - s_{k_l k_i}^{li} + u_{li} + v_{li}t_{k_i}^i + w_{li}\tau_{k_l}^l \leq 0 \\
& , \forall i \in \{1, ..., n\}, \forall\left(k_l, k_i\right) \in \{0, ..., K\}^2 && (35) \\
& q_l, r^l, s^l \geq 0 && (36)
\end{aligned}$$

From this dual we observe that only feasibility cuts are added as the variables μ do not appear in the objective function. Whenever $\xi_{k_l}^l = 0$, the objective coefficient for all the variables $r_{k_l k_i}^{li}$ is zero, meaning that we can make $r_{k_l k_i}^{li}$ tend to infinity and turn redundant the only constraint where said variable appears. The same phenomenon occurs with $\lambda_{k_i}^i = 0$ and the variables $s_{k_l k_i}^{li}$. Overall, when we are not cutting to solve the LP relaxation, for each pair (l, i) we will have only four non-redundant constraints and eight non-obviously zero variables r and s, leaving an LP of linear size in terms of n, K and p.

4 Computational speedups

4.1 Primal upper bounds: embedded heuristics

When using a cutting plane approach, it can be hard to decide when to stop. Of course, we can stop whenever we cannot separate the current incumbent, in which case it is feasible and the objective value of our master relaxed problem is that of the full approximated problem. However, waiting for full feasibility can - and does - make the method sloppy in practice. Any valid upper bound for the master problem can provide an optimality gap, therefore having some way to "repair" an incumbent (i.e. make it feasible for the full approximated problem) is of crucial importance. The main idea of our heuristics is similar to the arguments "by construction" of Propositions 3 and 6. For both models, we take the x components of the current incumbent, and solve the nonlinear approximated problems: 1)in $(u, v, \rho, \vartheta, \theta, \lambda, z, \xi, y)$ at x fixed for MINR, which can be done by hand by making constraints tight, and 2)in $(\rho, \lambda, z, \xi, y, \mu)$ at x fixed for CELL, where solving in $(\rho, \lambda, z, \xi, y, \mu)$ is also doable by hand, but solving in μ requires to solve p LPs with $O(n)$ variables and $O(n)$ constraints each.

4.2 Smart grids

From an implementation point of view, it is always interesting to use uniform grids from their simplicity. However, it is well known that better approximations can be constructed by choosing wisely the discretization points. We present here a way to cleverly a fixed number of points K out of the $\mathcal{K} \gg K$ points of a uniform grid, such that some error measure is minimized. In [1], they show how to select a subset of the $\mathcal{K}$ points - without any restriction on the size of the subset - such that the loss in precision plus some "storage cost" is minimized. They formulate the problem as a shortest path problem in a directed acyclic network with $\mathcal{K}$ nodes and $\mathcal{K}(\mathcal{K}-1)/2$ edges. The problem can be seen as a minimization problem taking the form $\min_{y \in \mathcal{Y}} \left\{ l^\top y + \alpha \cdot e^\top y \right\}$ where l and s are respectively a precision loss vector and a unitary weight vector e, the latter being ponderated by some penalization $\alpha \geq 0$. In their formulation, using more edges means selecting more points: the storage cost per point selected, α, is in fact a proxy to moderate the number of points selected. With this observation in mind, our objective is to minimize the same precision loss, while enforcing that the number of points selected is exactly some number K. The problem can be written as:

$$\min_{y \in \mathcal{Y}} \left\{ l^\top y : e^\top y = K \right\} .$$

Our main idea is to solve the latter problem via a Lagrangean algorithm that will select the best penalization α^* that will give a "good" selection - wrt to the precision loss l - of exactly K points. Given some penalization $\alpha > 0$, the lagrangean relaxation of our problem is

$$\min_{y \in \mathcal{Y}} \left\{ l^\top y + \alpha \cdot e^\top y \right\} - \alpha K .$$

If $\alpha = 0$, all the points are kept by the optimal solution of the lagrangean relaxation, whereas if α is very large, only the first and last point of the grid defined by the $\mathcal{K}$ points will be selected. In between, the number of points selected by the optimal solution will be monotone nonincreasing wrt to α. The main idea of our algorithm is to select the smallest α such that the optimal solution of the corresponding lagrangean relaxation uses exactly K points.

Moreover, in the multiple adversaries setting, for each variable x_i we use a single grid to approximate all the functions D_l^i for each $l \in [p]$. In consequence, we have to make sure that we are minimizing some kind of joint error amongst the adversaries. The easiest and most straightforward way to attain this goal was to minimize the sum of the errors induced by every function involving x_i.

5 Computational results

The algorithms presented in this paper were coded in C programming language and run over Dell PowerEdge C6420 cluster nodes with Intel Xeon Gold 6152 CPUs at 2.10GHz with 64Gb RAM each. All the Mixed Integer Linear Programming problems are solved using the callable library of CPLEX[7]. When generating the gradient and Benders cuts or building heuristic solutions from incumbents, we use the user cuts and callbacks technology of the callable library of CPLEX 12.6.

5.1 Parameters and instance generation

Parameters We solve all our problems at relative precision 10^{-9} in order to make sure that the cuts are taken into account and set a time limit of 3 hours for each run. During the Branch-and-Bound-and-Cut, we separate fractional incumbents only in the root node, and only integer incumbents during the tree search. The heuristics being very fast in practice, they are called each time an incumbent is found by the solver. K initial gradient cuts are added to approximate each of the convex real valued function.

Payoffs generation Although we do not assume zero sum games - i.e. the payoff of any attacker is equal to minus the payoff of the defender - it seems reasonable to assume that in practice, the payoffs should be somehow related. In this goal, we draw the payoffs R_i^l, $\bar{R}_i^l$, $-P_i^l$ and $-\bar{P}_i^l$ from a uniform distribution in $[0, 1]$.

Adversaries We test our algorithms with $p \in \{5, 7, 10, 12, 15\}$. The rationality coefficient λ^l of each attacker is drawn from a uniform distribution in $\lambda \cdot [0.9, 1.1]$, and we make vary $\lambda \in \{0.2, 0.7, 1.2, 1.7, 2.2\}$.

Defender's risk aversion The parameter α captures an absolute risk aversion and penalizes greatly defense strategies whose bad realizations exceed α. Noticing that α has units - the same as the payoffs - we selected the parameter α of the Entropic risk measure $\alpha \in \{0.1, 0.3, 0.5, 0.7, 0.9\} \subset [-1, 1]$. Notice that α is a very subjective measure of the risk aversion of the decision maker and as such, it can be difficult to adjust in practice.

Instance size and operational constraints We consider instances with a number of targets $n \in \{10, 20, 30, 40, 50\}$ and a number of resources $m = d \cdot n$ where $d \in \{0.1, 0.2, 0.3, 0.4, 0.5\}$. We consider only the case where only the resource constraint is present, without any operational ones.

Grids The approximation grids have K segments with $K \in \{2, 4, 8, 16, 32\}$. When using smart grids, we consider $\mathcal{K} = 256$ sampled points from which we select K.

Base case To analyze the influence of each parameter, we took as a base case $n = 20$, $m = 20 \cdot 0.3 = 6$, $p = 7$, $\alpha = 0.5$, $\lambda = 0.7$ and $K = 4$. We then vary n, d, p, α, λ and K independently and repeat the experiment 10 times.

5.2 Algorithmic performances

We test the MINR reformulation and the cell model (CELL) with uniform grids (U) or smart grids (S). For each experiment, we test the expected value maximization (EX) and the entropic risk minimization with $\alpha = 0.5$ (EN). For example, minimizing the entropic risk with the cell model using smart grids is denoted EN-CELL-S.

During the Branch and Bound and Cut procedure, let us define L as the best relaxation bound, U the objective value of the best (wrt the nonlinear mixed integer problems, where only the nonconvex functions are approximated) integer feasible solution, and R the real objective value of the best (wrt to the real, non approximated problem) solution so far. All the bounds found by each algorithm upon termination, L, U and R, are presented as the fraction of the best bound R^* found on the same instance by any algorithm.

General impression We show high level performance indicators in Table 2. Solving EN and EXP take similar execution times, however, the bounds and gaps are better for ENT (higher L, lower U and R). We can also see that MINR is faster and provides better bounds than CELL. Using smart grids makes the overall solution slightly slower for both algorithms and provides worse bounds for CELL but improves them for MINR. The process takes longer using smart grids because the

risk measure	EX				EN			
model	CELL		MINR		CELL		MINR	
grid	U	S	U	S	U	S	U	S
time	9171	9534	7436	7458	9364	9503	7232	7280
L	0.870	0.869	0.973	0.975	0.894	0.892	0.977	0.980
U	0.962	0.968	0.983	0.984	0.969	0.973	0.986	0.987
R	1.001	1.001	1.000	1.000	1.002	1.002	1.000	1.000
appGap	9.852	10.480	1.045	0.883	7.955	8.615	0.941	0.792
realGap	13.071	13.171	2.755	2.490	10.808	10.991	2.294	2.041

Table 2: Overall average normalized bounds. Time in seconds, gaps in %.

optimization problems become harder: in fact, selecting K points out of $\mathcal{K}$ for all the functions to approximate takes on average 4 seconds and 11 seconds in the worst case.

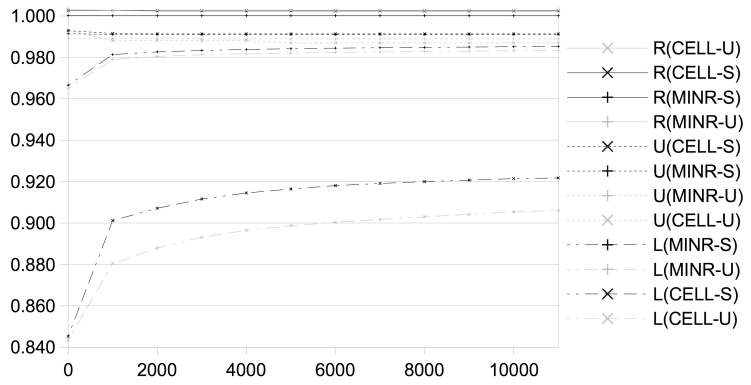

Fig. 1: Normalized bounds over time (in seconds) in the base case.

Parameters' influence In Table 3, we present the final gaps and the execution times in function of the parameters. The execution time steadily increases until reaching the limit of 3 hours (marked "*") with every parameter n, d, p, K, λ and α. We have the confirmation at a finer level that the MINR model outperforms CELL, and that the smart grids help to close the final gaps. More detailed results can be found in the Annex in Tables 7, 8, 9, 10, 11 and 12.

Example of bounds progress with time In Figure 1, we present an example of bound progression over time in the base case. It illustrates the fact that in terms of the relaxation bound L (dashed), LMINRP (+) is very superior to CELL (×) and that the smart grids (in black) do outperform the uniform grids (in gray). We can also confirm that in terms of real objective value R (solid) both algorithms are quite equivalent. More importantly the algorithms begin to stall after an hour, suggesting that the cut generation mechanisms in use might be improved

5.3 Qualitative results

Probability distribution calculation To compare a risk neutral defense policy with a risk averse one, we want to see if there is some kind of stochastic dominance of a risk averse strategy versus a risk neutral one. To do so, we compare the payoffs distributions of the defender depending on its risk aversion. In practice, the defender can cover m targets out of n and the attackers target a single place each. The only possible outcomes for the defender are: 1)being attacked on a defended target i by attacker l with payoff $V = \bar{R}_i^l > 0$ or 2)being attacked on an undefended target i by attacker l with payoff $V = \bar{P}_i^l < 0$. Consequently, if we assume that all the payoffs $\bar{R}_i^l$ and $\bar{P}_i^l$ are different the only values possible are in

$$V \in \{V_1 < V_2 < ... < V_{2np-1} < V_{2np}\} = \bigcup_{l=1}^{p} \bigcup_{i=1}^{n} \left\{ \bar{R}_i^l, \bar{P}_i^l \right\}.$$

r. m.		EX								EN							
alg.		CELL				MINR				CELL				MINR			
grid		U		S		U		S		U		S		U		S	
perf.		time	gap	time	gap	time	gap	time	gap	time	gap	time	gap	time	gap	time	gap
n	10	2498	1.775	5354	1.732	14	0.995	6	1.225	1287	1.499	2809	1.421	10	0.882	7	0.953
	20	*	8.293	*	8.895	3837	1.029	4387	1.249	*	6.154	*	6.500	5640	0.891	5479	0.973
	30	*	11.415	*	12.029	*	1.921	*	2.108	*	8.792	*	9.181	*	1.730	*	1.808
	40	*	12.979	*	13.240	*	2.449	*	2.655	*	11.592	*	11.543	10797	2.345	*	2.429
	50	*	13.662	*	13.733	*	2.699	*	2.979	*	12.433	*	12.433	*	2.670	*	2.751
d	0.1	783	1.667	2122	1.501	2	1.413	8	1.093	332	1.252	705	1.152	3	1.007	8	0.799
	0.2	*	4.902	*	5.474	183	1.170	785	0.648	8591	3.095	10361	3.461	287	0.784	1603	0.509
	0.3	*	8.293	*	8.895	3837	1.029	4387	1.249	*	6.154	*	6.500	5640	0.891	5479	0.973
	0.4	*	11.175	*	11.423	*	1.784	*	1.565	*	9.544	*	9.037	10161	1.404	10334	1.239
	0.5	*	11.566	*	11.651	*	1.642	*	1.575	*	10.836	*	11.576	*	1.961	*	1.519
p	5	*	7.822	*	8.216	1248	1.030	2132	1.236	*	5.474	*	5.670	1922	0.903	2560	0.965
	7	*	8.293	*	8.895	3837	1.029	4387	1.249	*	6.154	*	6.500	5640	0.891	5479	0.973
	10	*	9.334	*	9.636	10409	1.202	8866	1.258	*	7.141	*	7.710	*	1.171	9907	1.069
	12	*	9.992	*	10.081	*	1.870	*	1.382	*	8.619	*	8.615	*	1.750	10437	1.252
	15	*	11.478	*	11.698	*	2.817	*	1.685	*	9.846	*	9.937	*	2.463	*	1.729
K	2	909	8.786	3360	8.166	2	5.866	8	4.634	626	8.445	1864	7.924	3	4.287	8	3.542
	4	*	8.293	*	8.895	3837	1.029	4387	1.249	*	6.154	*	6.500	5640	0.891	5479	0.973
	8	*	13.004	*	13.157	*	0.914	*	0.740	*	11.332	*	11.459	*	0.807	*	0.716
	16	8035	13.872	8131	13.987	*	1.128	*	0.905	9505	12.771	8439	12.876	*	0.934	*	0.853
	32	10641	15.914	10763	14.602	*	1.215	*	0.975	*	14.682	10670	16.495	*	1.048	10761	0.944
λ	0.2	7743	0.521	8484	0.509	64	0.212	38	0.289	8567	0.300	8334	0.302	22	0.170	29	0.181
	0.7	*	8.293	*	8.895	3837	1.029	4387	1.249	*	6.154	*	6.500	5640	0.891	5479	0.973
	1.2	*	20.762	*	20.790	*	3.686	*	3.753	*	18.609	*	18.631	*	3.773	*	3.387
	1.7	*	37.306	*	37.440	*	8.423	*	7.667	*	36.022	*	35.908	*	8.679	*	7.408
	2.2	*	48.272	*	48.624	*	14.400	*	12.667	*	47.343	*	47.604	*	14.365	*	12.443
α	0.1	-	-	-	-	-	-	-	-	*	5.022	*	5.678	3968	0.596	2022	0.600
	0.3	-	-	-	-	-	-	-	-	*	5.939	*	5.938	3905	0.809	3552	0.859
	0.5	-	-	-	-	-	-	-	-	*	6.154	*	6.500	5640	0.891	5479	0.973
	0.7	-	-	-	-	-	-	-	-	*	6.656	*	6.702	6829	0.950	7808	1.033
	0.9	-	-	-	-	-	-	-	-	*	6.792	*	7.029	7672	0.967	9496	1.067

Table 3: Execution time (seconds) and final gaps (%) Vs. parameters. "*"= 3h time out. "-"= no EXP for α experiments.

Recall from Section 2 that given a mixed defense strategy $x \in [0,1]^n$ and the associated QR $y(x) \in [0,1]^n$, the payoff of the defender is:

$$\begin{array}{ll} \bar{P}_i^l & \text{with probability } \pi^l y_i^l(x)(1-x_i) \\ \bar{R}_i^l & \text{with probability } \pi^l y_i^l(x) x_i \ . \end{array}$$

This way we can compute the probability distribution of the payoff of any defender without sampling a large number of simulations. We compare the expected value, variance, Value at Risk (VaR) at level 10%, Conditional Value at Risk (CVaR) at level 10% and entropic risk at level $\alpha' = 0.5$ in function of α and λ.

General comments We now compare all the solutions obtained with MINR-S, as the solutions it provides showed to be the most reliable. All the indicators are given as the fraction of the same indicator for the risk neutral solution with the base case parameter.

There is no clear influence of the parameters n, p and the number of breakpoints K. However, the remaining parameters do have a strong influence on the characteristics of a risk averse solution.

α *influence* In Table 4, we can see that by decreasing α (i.e. getting more risk averse), there is a clear improvement in terms of all the risk aversion indicators. That can come, however, at the cost of a significant loss in expected payoff.

risk m.	$E_{\alpha=0.1}$	$E_{\alpha=0.3}$	$E_{\alpha=0.5}$	$E_{\alpha=0.7}$	$E_{\alpha=0.9}$	$\mathbb{E}$
$\mathbb{E}$	1.294	1.108	1.048	1.027	1.019	1
$\mathbb{V}$	0.840	0.881	0.919	0.939	0.949	1
VaR_{10}	0.954	0.952	0.972	0.985	0.991	1
CVaR_{10}	0.957	0.973	0.985	0.990	0.991	1
$E_{0.5}$	1.029	0.981	0.978	0.980	0.983	1

Table 4: Quality Vs. α. All indicators are losses.

λ *influence* In Table 5, we can see that facing increasingly rational adversaries has a significant negative impact on the risk neutral solution, whereas the risk averse solutions hedge welll against smarter ennemies.

λ	0.2		0.7		1.2		1.7		2.2	
risk m.	ENT	EXP	ENT	EXP	ENT	EXP	ENT	EXP	ENT	EXP
$\mathbb{E}$	0.979	0.921	1.048	1	1.061	1.013	1.070	1.016	1.096	1.019
$\mathbb{V}$	0.926	1.033	0.920	1	0.912	0.986	0.893	0.972	0.854	0.971
VaR_{10}	0.952	0.994	0.973	1	0.976	0.998	0.966	0.998	0.955	0.999
CVaR_{10}	0.974	0.992	0.985	1	0.987	1.001	0.983	0.999	0.977	0.999
$E_{0.5}$	0.952	0.977	0.979	1	0.981	1.000	0.975	0.995	0.966	0.995

Table 5: Quality Vs. λ. All indicators are losses.

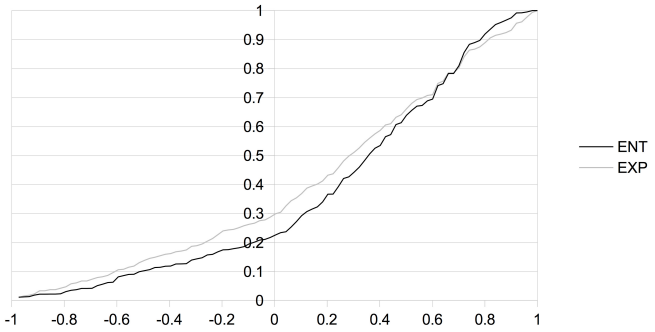

Fig. 2: Cumulative distributions of the *loss* for $x\,(E_{0.5})$ (black) and $x\,(\mathbb{E})$ (gray)

d influence In Table 6, we can observe - without surporise - that having more resources (higher values of d) has an extremely strong impact on the quality of the solution: in fact, when we are able to cover simultaneously half the targets ($d = 0.5$), the expected losses of both the risk averse and risk neutral policies become negative.

d	0.1		0.2		0.3		0.4		0.5	
risk m.	ENT	EXP	ENT	EXP	ENT	EXP	ENT	EXP	ENT	EXP
$\mathbb{E}$	2.122	2.105	1.590	1.546	1.048	1	0.524	0.457	-0.027	-0.088
$\mathbb{V}$	0.568	0.608	0.761	0.834	0.92	1	1.009	1.095	1.052	1.128
VaR_{10}	1.036	1.048	1.008	1.022	0.973	1	0.923	0.963	0.872	0.913
CVaR_{10}	1.018	1.023	1.001	1.012	0.985	1	0.96	0.985	0.933	0.963
$E_{0.5}$	1.262	1.271	1.124	1.138	0.979	1	0.82	0.844	0.641	0.669

Table 6: Quality Vs. d. All indicators are losses.

Example of distributions E_α Vs. $\mathbb{E}$ In Figure 2, we compare the cumulative distributions of a risk averse solution (black) and that of a risk neutral solution (gray). We can see that past the *loss* 0.7, the risk averse solution dominates the risk averse one. The variance of the risk averse solution is 20% lower at the cost of losing a 30% in payoff.

6 Conclusions

In this paper, we extended the classic model of Stackelberg security games with quantal response to a risk averse setting for the defender and facing several adversaries with different degrees of rationality. We presented two ways of finding an approximately optimal defense strategy by solving nonlinear MIPs via cutting planes. The first methodology (CELL) has a broader range of applications, but the second (MINR) is more efficient, both in solution quality and execution time, and offers a reasonable performance for practical mid-sized cases. Computational results showed that minimizing an Entropic risk measure instead of maximizing

the expected value can be advantageous from a qualitative point of view, allowing to significantly reduce the overall payoff variance and the probability of bad scenarios to occur.

Being cutting planes methods, our algorithms suffered from a sloppy behavior towards the end of the tree search. In a future work, we should investigate the use of stronger cuts, stabilization methods, or the fine tuning of the cut generation process. The Entropic risk measure is not the only way to introduce risk aversion in the behavior of an agent: In fact, there is a whole array of risk aversion-inducing tools in the literature that can be used instead. In a current work, we show that using classical risk measures such as Value-at-Risk, Conditional-Value-at-Risk, upper semi-deviations, etc... the resulting optimization problems have the same structure as the ones described in this paper.

Acknowledgements Powered@NLHPC: This research was partially supported by the supercomputing infrastructure of the NLHPC (ECM-02) and funded by Conicyt through grant FONDEF No. D10I1002.

References

1. Ahuja, R., Magnanti, T., Orlin, J.: Network flows: theory, algorithms, and applications. Prentice hall (1993)
2. Benders, J.: Partitioning procedures for solving mixed-variables programming problems. Numerische Mathematik **4**(1), 238–252 (1962)
3. Bier, V.M.: Choosing what to protect. Risk Analysis **27**(3), 607–620 (2007)
4. Brown, G., Carlyle, M., Salmerón, J., Wood, K.: Defending critical infrastructure. Interfaces **36**(6), 530–544 (2006)
5. Camerer, C., Ho, T.H., Chong, J.K.: A cognitive hierarchy model of games. The Quarterly Journal of Economics **119**(3), 861–898 (2004)
6. Chicoisne, R., Ordóñez, F.: Risk averse stackelberg security games with quantal response. In: Proceedings of GameSec 2016, New York, vol. LNCS 9996, pp. 83–100 (2016)
7. CPLEX: V12. 1: User Manual for CPLEX (2009)
8. Gilbert, E.: Gray codes and paths on the n-cube. Bell System Technical Journal **37**(3), 815–826 (1958)
9. Haile, P., Hortaçsu, A., Kosenok, G.: On the empirical content of quantal response equilibrium. The American Economic Review **98**(1), 180–200 (2008)
10. Harsanyi, J.C.: Games with incomplete information played by "bayesian" players, i-iii: Part i. the basic model. Management Science **14**(3), 159–182 (1967)
11. Jiang, A.X., Yin, Z., Kietkintveld, C., Leyton-Brown, K., Sandholm, T., Tambe, M.: Towards optimal patrol strategies for fare inspection in transit systems. In: Proc. of the AAAI Spring Symposium on Game Theory for Security, Sustainability and Health (2012)
12. Kar, D., Nguyen, T.H., Fang, F., Brown, M., Sinha, A., Tambe, M., Jiang, A.X.: Trends and applications in stackelberg security games. In: T. Basar, G. Zaccour (eds.) Handbook of Dynamic Game Theory. Springer, Cham (2016)
13. Kiekintveld, C., Jain, M., Tsai, J., Pita, J., Ordóñez, F., Tambe, M.: Computing optimal randomized resource allocations for massive security games. In: Proceedings of the 8th AAMAS Conference, Budapest, Hungary, vol. 1, pp. 689–696. International Foundation for AAMAS (2009)
14. Knuth, D.E.: The art of computer programming: sorting and searching, vol. 3. Pearson Education (1998)
15. McKelvey, R., Palfrey, T.: Quantal response equilibria for normal form games. Games and economic behavior **10**(1), 6–38 (1995)
16. Pita, J., Jain, M., Marecki, J., Ordóñez, F., Portway, C., Tambe, M., Western, C., Paruchuri, P., Kraus, S.: Deployed armor protection: the application of a game theoretic model for security at the los angeles international airport. In: Proceedings of the 7th AAMAS: industrial track, Cascais Miragem, Portugal, pp. 125–132. International Foundation for AAMAS (2008)

17. Pita, J., Jain, M., Ordóñez, F., Tambe, M., Kraus, S.: Solving stackelberg games in the real-world: Addressing bounded rationality and limited observations in human preference models. Artificial Intelligence Journal **174**(15), 1142–1171 (2010)
18. Pratt, J.W.: Risk aversion in the small and in the large. Econometrica: Journal of the Econometric Society **32**(1/2), 122–136 (1964)
19. Rovatti, R., DAmbrosio, C., Lodi, A., Martello, S.: Optimistic milp modeling of non-linear optimization problems. European Journal of Operational Research **239**(1), 32–45 (2014)
20. Shieh, E., An, B., Yang, R., Tambe, M., Baldwin, C., DiRenzo, J., Maule, B., Meyer, G.: PROTECT: A deployed game theoretic system to protect the ports of the United States. In: Proc. of The 11th International Conference on Autonomous Agents and Multiagent Systems (AAMAS) (2012)
21. Stahl II, D., Wilson, P.: Experimental evidence on players' models of other players. Journal of economic behavior & organization **25**(3), 309–327 (1994)
22. Thakur, L.S.: Error analysis for convex separable programs: the piecewise linear approximation and the bounds on the optimal objective value. SIAM Journal on Applied Mathematics **34**(4), 704–714 (1978)
23. Tsai, J., Rathi, S., Kiekintveld, C., Ordóñez, F., Tambe, M.: IRIS: a tool for strategic security allocation in transportation networks. In: Proc. of The 8th International Conference on Autonomous Agents and Multiagent Systems (AAMAS), pp. 37–44 (2009)
24. Vielma, J., Nemhauser, G.: Modeling disjunctive constraints with a logarithmic number of binary variables and constraints. Mathematical Programming **128**(1-2), 49–72 (2011)
25. Von Stackelberg, H.: The theory of the market economy. William Hodge (1952)
26. Wright, J., Leyton-Brown, K.: Beyond equilibrium: Predicting human behavior in normal-form games. In: Proceedings of the 24th AAAI conference on artificial intelligence, Atlanta, GA (2010)
27. Yang, R., Kiekintveld, C., Ordóñez, F., Tambe, M., John, R.: Improving resource allocation strategy against human adversaries in security games. In: 22th IJCAI Proceedings, Barcelona, Spain, vol. 22, pp. 458–464. AAAI Press (2011)
28. Yang, R., Ordóñez, F., Tambe, M.: Computing optimal strategy against quantal response in security games. In: Proceedings of the 11th AAMAS, Valencia, Spain, vol. 2, pp. 847–854. International Foundation for AAMAS (2012)

7 Annex

In Tables 7, 8, 9, 10, 11 and 12 we present the full bounds over all the parameters.

risk measure			EX				EN			
model			CELL		MINR		CELL		MINR	
grid			U	S	U	S	U	S	U	S
time	n	10	2498	5354	14	6	1287	2809	10	7
		20	*	*	3837	4387	*	*	5640	5479
		30	*	*	*	*	*	*	*	*
		40	*	*	*	*	*	*	10797	*
		50	*	*	*	*	*	*	*	*
L	n	10	0.983	0.983	0.990	0.988	0.986	0.986	0.991	0.990
		20	0.918	0.912	0.990	0.988	0.940	0.937	0.991	0.990
		30	0.887	0.881	0.981	0.979	0.915	0.912	0.983	0.982
		40	0.872	0.869	0.976	0.973	0.887	0.888	0.977	0.976
		50	0.865	0.864	0.973	0.970	0.879	0.879	0.973	0.972
U	n	10	0.983	0.984	0.990	0.988	0.986	0.986	0.991	0.991
		20	0.983	0.984	0.990	0.988	0.985	0.987	0.991	0.990
		30	0.984	0.986	0.990	0.988	0.986	0.989	0.991	0.991
		40	0.984	0.986	0.990	0.988	0.988	0.989	0.991	0.991
		50	0.986	0.988	0.990	0.988	0.990	0.991	0.991	0.991
R	n	10	1.001	1.000	1.000	1.000	1.001	1.001	1.000	1.000
		20	1.001	1.001	1.000	1.000	1.002	1.002	1.000	1.000
		30	1.002	1.002	1.000	1.000	1.003	1.004	1.000	1.000
		40	1.002	1.002	1.000	1.000	1.004	1.004	1.000	1.000
		50	1.002	1.002	1.000	1.000	1.004	1.004	1.000	1.000
appGap	n	10	0.010	0.102	0.010	0.010	0.010	0.010	0.010	0.009
		20	6.557	7.321	0.010	0.015	4.542	5.030	0.010	0.017
		30	9.835	10.639	0.935	0.900	7.199	7.777	0.873	0.871
		40	11.450	11.881	1.459	1.453	10.177	10.266	1.479	1.494
		50	12.237	12.462	1.708	1.776	11.196	11.258	1.806	1.821
realGap	n	10	1.775	1.732	0.995	1.225	1.499	1.421	0.882	0.953
		20	8.293	8.895	1.029	1.249	6.154	6.500	0.891	0.973
		30	11.415	12.029	1.921	2.108	8.792	9.181	1.730	1.808
		40	12.979	13.240	2.449	2.655	11.592	11.543	2.345	2.429
		50	13.662	13.733	2.699	2.979	12.433	12.433	2.670	2.751

Table 7: Performances Vs. n. "*"= 3h time out

risk measure			EX				EN			
model			CELL		MINR		CELL		MINR	
grid			U	S	U	S	U	S	U	S
time	d	0.1	783	2122	2	8	332	705	3	8
		0.2	*	*	183	785	8591	10361	287	1603
		0.3	*	*	3837	4387	*	*	5640	5479
		0.4	*	*	*	*	*	*	10161	10334
		0.5	*	*	*	*	*	*	*	*
L	d	0.1	0.984	0.986	0.986	0.989	0.988	0.989	0.990	0.992
		0.2	0.952	0.946	0.988	0.994	0.971	0.967	0.992	0.995
		0.3	0.918	0.912	0.990	0.988	0.940	0.937	0.991	0.990
		0.4	0.889	0.887	0.982	0.984	0.906	0.911	0.986	0.988
		0.5	0.885	0.884	0.984	0.984	0.893	0.886	0.981	0.985
U	d	0.1	0.984	0.986	0.986	0.989	0.989	0.990	0.990	0.992
		0.2	0.982	0.984	0.988	0.994	0.986	0.987	0.992	0.995
		0.3	0.983	0.984	0.990	0.988	0.985	0.987	0.991	0.990
		0.4	0.986	0.986	0.985	0.988	0.987	0.988	0.989	0.991
		0.5	0.990	0.990	0.993	0.990	0.990	0.990	0.994	0.992
R	d	0.1	1.001	1.001	1.000	1.000	1.001	1.001	1.000	1.000
		0.2	1.001	1.001	1.000	1.000	1.002	1.001	1.000	1.000
		0.3	1.001	1.001	1.000	1.000	1.002	1.002	1.000	1.000
		0.4	1.001	1.001	1.000	1.000	1.002	1.002	1.000	1.000
		0.5	1.001	1.001	1.000	1.000	1.002	1.002	1.000	1.000
appGap	d	0.1	0.010	0.010	0.010	0.010	0.010	0.010	0.010	0.010
		0.2	3.075	3.836	0.010	0.010	1.544	2.086	0.010	0.010
		0.3	6.557	7.321	0.010	0.015	4.542	5.030	0.010	0.017
		0.4	9.776	10.108	0.274	0.402	8.168	7.745	0.301	0.368
		0.5	10.635	10.651	0.923	0.616	9.787	10.544	1.320	0.694
realGap	d	0.1	1.667	1.501	1.413	1.093	1.252	1.152	1.007	0.799
		0.2	4.902	5.474	1.170	0.648	3.095	3.461	0.784	0.509
		0.3	8.293	8.895	1.029	1.249	6.154	6.500	0.891	0.973
		0.4	11.175	11.423	1.784	1.565	9.544	9.037	1.404	1.239
		0.5	11.566	11.651	1.642	1.575	10.836	11.576	1.961	1.519

Table 8: Performances Vs. d. "*"= 3h time out

risk measure			EX				EN			
model			CELL		MINR		CELL		MINR	
grid			U	S	U	S	U	S	U	S
time	p	5	*	*	1248	2132	*	*	1922	2560
		7	*	*	3837	4387	*	*	5640	5479
		10	*	*	10409	8866	*	*	*	9907
		12	*	*	*	*	*	*	*	10437
		15	*	*	*	*	*	*	*	*
L	p	5	0.923	0.919	0.990	0.988	0.947	0.945	0.991	0.990
		7	0.918	0.912	0.990	0.988	0.940	0.937	0.991	0.990
		10	0.908	0.904	0.988	0.987	0.930	0.925	0.988	0.989
		12	0.901	0.900	0.981	0.986	0.915	0.915	0.983	0.987
		15	0.886	0.884	0.972	0.983	0.903	0.902	0.975	0.983
U	p	5	0.983	0.985	0.990	0.988	0.987	0.988	0.991	0.990
		7	0.983	0.984	0.990	0.988	0.985	0.987	0.991	0.990
		10	0.983	0.983	0.990	0.988	0.984	0.986	0.991	0.990
		12	0.983	0.984	0.990	0.988	0.985	0.986	0.991	0.990
		15	0.984	0.985	0.990	0.988	0.985	0.986	0.991	0.990
R	p	5	1.002	1.002	1.000	1.000	1.002	1.002	1.000	1.000
		7	1.001	1.001	1.000	1.000	1.002	1.002	1.000	1.000
		10	1.001	1.001	1.000	1.000	1.002	1.002	1.000	1.000
		12	1.001	1.001	1.000	1.000	1.002	1.002	1.000	1.000
		15	1.000	1.001	1.000	1.000	1.001	1.001	1.000	1.000
appGap	p	5	6.095	6.613	0.010	0.010	4.010	4.364	0.010	0.010
		7	6.557	7.321	0.010	0.015	4.542	5.030	0.010	0.017
		10	7.623	8.021	0.195	0.029	5.482	6.198	0.282	0.089
		12	8.396	8.558	0.901	0.154	7.112	7.181	0.853	0.269
		15	9.955	10.317	1.865	0.460	8.355	8.527	1.581	0.749
realGap	p	5	7.822	8.216	1.030	1.236	5.474	5.670	0.903	0.965
		7	8.293	8.895	1.029	1.249	6.154	6.500	0.891	0.973
		10	9.334	9.636	1.202	1.258	7.141	7.710	1.171	1.069
		12	9.992	10.081	1.870	1.382	8.619	8.615	1.750	1.252
		15	11.478	11.698	2.817	1.685	9.846	9.937	2.463	1.729

Table 9: Performances Vs. p. "*"= 3h time out

risk measure			EX				EN			
model			CELL		MINR		CELL		MINR	
grid			U	S	U	S	U	S	U	S
time	K	2	909	3360	2	8	626	1864	3	8
		4	*	*	3837	4387	*	*	5640	5479
		8	*	*	*	*	*	*	*	*
		16	8035	8131	*	*	9505	8439	*	*
		32	10641	10763	*	*	*	10670	*	10761
L	K	2	0.914	0.920	0.942	0.954	0.920	0.925	0.958	0.965
		4	0.918	0.912	0.990	0.988	0.940	0.937	0.991	0.990
		8	0.871	0.869	0.991	0.992	0.888	0.887	0.992	0.993
		16	0.862	0.861	0.988	0.991	0.874	0.874	0.990	0.991
		32	0.842	0.855	0.988	0.990	0.857	0.839	0.989	0.990
U	K	2	0.914	0.920	0.942	0.955	0.920	0.925	0.958	0.966
		4	0.983	0.984	0.990	0.988	0.985	0.987	0.991	0.990
		8	0.998	0.998	0.997	0.997	0.999	1.000	0.997	0.998
		16	1.000	1.001	0.999	0.999	1.002	1.002	0.999	0.999
		32	1.002	1.001	1.000	1.000	1.004	1.004	1.000	1.000
R	K	2	1.002	1.002	1.001	1.001	1.005	1.004	1.001	1.001
		4	1.001	1.001	1.000	1.000	1.002	1.002	1.000	1.000
		8	1.001	1.001	1.000	1.000	1.002	1.002	1.000	1.000
		16	1.001	1.001	1.000	1.000	1.002	1.003	1.000	1.000
		32	1.002	1.002	1.000	1.000	1.004	1.004	1.000	1.000
appGap	K	2	0.010	0.010	0.009	0.010	0.009	0.009	0.009	0.010
		4	6.557	7.321	0.010	0.015	4.542	5.030	0.010	0.017
		8	12.726	12.879	0.587	0.457	11.043	11.220	0.563	0.514
		16	13.816	13.938	1.055	0.846	12.724	12.832	0.891	0.817
		32	15.902	14.593	1.204	0.968	14.684	16.495	1.048	0.942
realGap	K	2	8.786	8.166	5.866	4.634	8.445	7.924	4.287	3.542
		4	8.293	8.895	1.029	1.249	6.154	6.500	0.891	0.973
		8	13.004	13.157	0.914	0.740	11.332	11.459	0.807	0.716
		16	13.872	13.987	1.128	0.905	12.771	12.876	0.934	0.853
		32	15.914	14.602	1.215	0.975	14.682	16.495	1.048	0.944

Table 10: Performances Vs. K. "*"= 3h time out

risk measure			EX				EN			
model			CELL		MINR		CELL		MINR	
grid			U	S	U	S	U	S	U	S
time	λ	0.2	7743	8484	64	38	8567	8334	22	29
		0.7	*	*	3837	4387	*	*	5640	5479
		1.2	*	*	*	*	*	*	*	*
		1.7	*	*	*	*	*	*	*	*
		2.2	*	*	*	*	*	*	*	*
L	λ	0.2	0.995	0.995	0.998	0.997	0.997	0.997	0.998	0.998
		0.7	0.918	0.912	0.990	0.988	0.940	0.937	0.991	0.990
		1.2	0.793	0.793	0.963	0.963	0.816	0.815	0.963	0.966
		1.7	0.628	0.626	0.916	0.924	0.643	0.644	0.914	0.926
		2.2	0.518	0.514	0.856	0.874	0.530	0.527	0.857	0.876
U	λ	0.2	1.000	1.000	0.998	0.997	1.000	1.000	0.998	0.998
		0.7	0.983	0.984	0.990	0.988	0.985	0.987	0.991	0.990
		1.2	0.967	0.972	0.973	0.972	0.967	0.972	0.976	0.976
		1.7	0.838	0.866	0.948	0.953	0.845	0.874	0.953	0.958
		2.2	0.694	0.752	0.915	0.934	0.699	0.763	0.921	0.938
R	λ	0.2	1.000	1.000	1.000	1.000	1.000	1.000	1.000	1.000
		0.7	1.001	1.001	1.000	1.000	1.002	1.002	1.000	1.000
		1.2	1.001	1.001	1.000	1.000	1.002	1.002	1.000	1.000
		1.7	1.001	1.001	1.000	1.000	1.004	1.005	1.001	1.000
		2.2	1.001	1.001	1.000	1.001	1.006	1.005	1.001	1.000
appGap	λ	0.2	0.471	0.460	0.010	0.010	0.264	0.268	0.010	0.010
		0.7	6.557	7.321	0.010	0.015	4.542	5.030	0.010	0.017
		1.2	17.947	18.375	0.999	0.936	15.668	16.091	1.374	1.022
		1.7	25.097	27.701	3.352	3.050	23.983	26.329	4.067	3.326
		2.2	25.278	31.597	6.418	6.424	24.221	31.014	6.881	6.599
realGap	λ	0.2	0.521	0.509	0.212	0.289	0.300	0.302	0.170	0.181
		0.7	8.293	8.895	1.029	1.249	6.154	6.500	0.891	0.973
		1.2	20.762	20.790	3.686	3.753	18.609	18.631	3.773	3.387
		1.7	37.306	37.440	8.423	7.667	36.022	35.908	8.679	7.408
		2.2	48.272	48.624	14.400	12.667	47.343	47.604	14.365	12.443

Table 11: Performances Vs. λ. "*"= 3h time out

model			CELL		MINR	
grid			U	S	U	S
time	α	0.1	*	*	3968	2022
		0.3	*	*	3905	3552
		0.5	*	*	5640	5479
		0.7	*	*	6829	7808
		0.9	*	*	7672	9496
L	α	0.1	0.952	0.946	0.994	0.994
		0.3	0.943	0.943	0.992	0.991
		0.5	0.940	0.937	0.991	0.990
		0.7	0.935	0.935	0.991	0.990
		0.9	0.934	0.931	0.990	0.989
U	α	0.1	0.991	0.992	0.995	0.994
		0.3	0.988	0.989	0.992	0.992
		0.5	0.985	0.987	0.991	0.990
		0.7	0.985	0.986	0.991	0.990
		0.9	0.984	0.986	0.991	0.990
R	α	0.1	1.003	1.003	1.000	1.000
		0.3	1.002	1.003	1.000	1.000
		0.5	1.002	1.002	1.000	1.000
		0.7	1.002	1.002	1.000	1.000
		0.9	1.002	1.002	1.000	1.000
appGap	α	0.1	3.914	4.641	0.034	0.010
		0.3	4.574	4.657	0.010	0.010
		0.5	4.542	5.030	0.010	0.017
		0.7	5.056	5.242	0.043	0.049
		0.9	5.145	5.568	0.051	0.084
realGap	α	0.1	5.022	5.678	0.596	0.600
		0.3	5.939	5.938	0.809	0.859
		0.5	6.154	6.500	0.891	0.973
		0.7	6.656	6.702	0.950	1.033
		0.9	6.792	7.029	0.967	1.067

Table 12: Performances Vs. α. "*"= 3h time out